Iterative Learning Control in Health Care

ELECTRICAL STIMULATION AND ROBOTIC-ASSISTED UPPER-LIMB STROKE REHABILITATION

CHRIS T. FREEMAN, ERIC ROGERS, ANN-MARIE HUGHES, JANE H. BURRIDGE, and KATIE L. MEADMORE

xxxxxxxxx

Annually, 15 million people worldwide suffer a stroke, and 5 million are left permanently disabled. A stroke is usually caused when a blood clot blocks a vessel in the brain and acts like a dam, stopping the blood reaching the regions downstream. Alternatively, it may be caused by a hemorrhage, in which a vessel ruptures and leaks blood into surrounding areas. As a result, some of the connecting nerve cells die, and the person commonly suffers partial paralysis on one side of the body, termed hemiplegia. Cells killed in this way cannot regrow, but the brain has some spare capacity and, hence, new connections can be made. The brain is continually and rapidly changing as new skills are learned, new connections are formed, and redundant ones

disappear. A person who relearns skills after a stroke goes through the same process as someone learning to play tennis or a baby learning to walk, requiring sensory feedback during the repeated practice of a task. Unfortunately, the problem is that they can hardly move and, therefore, do not receive feedback on their performance.

Stroke survivors often have a complex pattern of upper-limb motor impairments, resulting in a loss of functional abilities such as reaching. The relationship between reaching and independence is reflected in measures of functional independence, such as the Barthel index [1] where the ability to reach is required for over half of the activity of daily living tasks. The current prognosis for upper-limb recovery following a stroke is poor, with a review reporting that complete recovery occurs in less than 15% of patients with initial paralysis [2]. Stroke is also an age-related disease [3], placing an increasing burden on long-term health

and related resources unless improvements are made in achieving independence. Consequently, there is a pressing need to improve the effectiveness of treatments. Enabling rehabilitation outside the hospital, supported by mobile technology, may lead to reduced cost, increased intensity of therapy, and a shift in the emphasis of responsibility for good health from health professionals to patients.

Research into conventional therapy and motor learning theory provides evidence that the intensity of practice of a task and feedback are important [4]–[7]. This knowledge is motivating the development of novel treatments such as robotic therapy that provide the opportunity for repetitive movement practice. Although the use of robotic therapy in upper-limb rehabilitation is relatively recent, reviews of the literature suggest that robot-aided therapy improves motor control of the proximal upper limb and may improve functional outcomes [8], [9]. Moreover, electromechanical and robotic devices may have an advantage over conventional therapies in the frequency of movement repetitions because of an increased motivation to train and the opportunity for independent exercise [8]. Based on existing evidence, use of rehabilitation robots is recommended in the U.K. stroke guidelines [10].

Clinical evidence exists to support the therapeutic use of functional electrical stimulation (FES) to improve motor control [11]. FES makes muscles work by causing electrical impulses to travel along the nerves in much the same way as electrical impulses from the brain, and if stimulation is carefully controlled, a useful movement can be made. Theoretical results from neurophysiology [12] and motor learning research [13] support clinical research with the conclusion that the therapeutic benefit of stimulation is maximized when applied coincidently with a patient's own voluntary intention to move [14]. A hypothesis is proposed in [15] to explain the added benefit of increased recovery when FES is used to mimic a weak or paralyzed movement, describing how the anterior horn (AH) cell synapses may be strengthened by receiving simultaneous impulses along the motor nerves due to FES and voluntary effort, and thereby allowing AH cells to compensate for damage to the subject's motor system. This hypothesis explains why the increased degree of functional recovery is closely related to the accuracy of the stimulation applied to assist the subject's own voluntary completion of a task.

A variety of FES model-based control methods have been employed to control movement [16], however, the majority are intended for spinal cord injury (SCI) subjects, which is reflected in the number of approaches focused on the lower limb. A contributing factor to the far greater number of FES schemes available for the lower limb is the simplicity of the musculoskeletal system compared with the upper limb, and the relative ease of muscle selectivity and recruitment. Examples include optimal [17], H_∞ [18], and fuzzy [19] control of standing, sliding mode control of shank movement [20], data-driven control [21] of the knee

joint, and multichannel proportional integral derivative (PID) control of the wrist [22]. Artificial neural networks have been applied to both the upper [23], [24] and lower limbs [25] of paretic subjects, although disadvantages to the approach have been reported [26].

Advanced techniques, such as those referenced above, have rarely transferred to clinical practice [27], especially in the case of stroke rehabilitation, where the strategies adopted are either open loop or the stimulation is triggered using limb position or electromyographic (EMG) signals to provide a measure of participant's intended movement [28]–[30]. Closed-loop control has been achieved using EMG [31], but this has not been incorporated in model-based controllers since EMG does not directly relate to the force or torque generated by the muscle. In the few cases where model-based control approaches have been used clinically, they have enabled a far higher level of tracking accuracy.

A principal reason for the lack of model-based methods finding application in a program of patient trials is the difficulty in obtaining reliable biomechanical models. In the clinical setting there is minimal set-up time, reduced control over environmental constraints, and little possibility of repeating any one test in the program of treatment undertaken; controllers are required to perform to a minimum standard on a wide number of subjects and conditions. Moreover the underlying musculoskeletal system is highly sensitive to physiological conditions, including skin impedance, temperature, and moisture and electrode placement, in addition to time-varying effects such as spasticity and fatigue [32]. These problems are often exacerbated in the case of stroke because hemiplegic subjects exhibit both voluntary and involuntary responses to applied stimulation. The limited number of model-based approaches that have been used in stroke rehabilitation therefore provide limited scope to adapt the applied stimulation to changes in the underlying system due to fatigue or spasticity, leading to reduction in performance and an inability to fully exploit the therapeutic potential.

Iterative learning control (ILC) is one model-based approach to stroke rehabilitation that has progressed to a program of clinical trials, which constitute the first major stage towards the eventual transfer into practice. In contrast to other approaches employed to control FES, ILC exploits the repeating nature of the patients' tasks to improve performance by learning from past experience. By updating the control input using data collected over previous attempts at the task, ILC is able to respond to physiological changes in the system, such as spasticity and the presence of a patient's voluntary effort, which would otherwise erode performance. ILC can also closely regulate the amount of stimulation supplied, ensuring that minimum assistance is provided thereby promoting the patient's maximum voluntary contribution to the task completion. As the treatment progresses, this control action encourages

patients to exert an increasing voluntary effort with each trial and a corresponding decrease in the level of FES applied.

In an initial feasibility study, FES was applied to generate torque about the elbow joint, and ILC was used to update the stimulation level to assist a patient's completion of a planar reaching task. To enable accurate performance, dynamic models of the arm [33] were developed, together with model-based ILC schemes [34]. Clinical trials produced statistically significant results across a range of outcome measures that showed impairment in arm function reduced over the course of 18 treatment sessions [35], thereby establishing the effectiveness of the approach.

Unsurprisingly, the improvement in motor function in this clinical trial is only significant across tasks similar to those trained during treatment. This motivates ongoing development of a rehabilitation system using ILC to assist unconstrained three-dimensional (3-D) movement through FES applied to a greater number of muscles, again with clinical trials. Further improvements in outcome measures will increase the recognition of ILC as a significant advance by end users, that is, practitioners in health care. This research will also contribute to establishing the use of ILC within rehabilitation, with research already emerging from other groups, such as [36]–[38], in the area of lower-limb robotic rehabilitation. The clinical trials are among the first to use advanced FES controllers and to combine both robotics and electrical stimulation for the purpose of stroke rehabilitation.

This article describes the application of ILC in upper-limb stroke rehabilitation, focusing first on the planar robotic system in which the development of a biomechanical model and subsequent design of ILC is described. Results are reported from a clinical trial where these ILC schemes were employed to assist movement tasks with stroke patients, together with a discussion of the outcome measures used by physiotherapists to assess the effect of rehabilitation therapy. Having confirmed feasibility, ongoing research on a 3-D system to train unconstrained upper-limb movements is described, which involves a substantial extension of the underlying ILC framework to significantly increase the potential of rehabilitation. This article also summarizes clinical results from a recent further program of trials with stroke patients, and concludes with a discussion of the limitations and areas of future research into the use of ILC in stroke rehabilitation.

ILC-BASED STROKE REHABILITATION FOR PLANAR TASKS

Relearning skills after a stroke requires a person to practice movements by repetition and use feedback from previous attempts to improve the next one. The problem is that practice is limited, or impossible, due to the effects of the stroke, which means stroke patients do not receive sensory-motor feedback of performance, such as sight, touch, and joint position sense. When applying stimulation to overcome this problem, a suitable strategy is for the patient to attempt to complete a prescribed tracking task over a finite duration, performance to be measured, and the resulting information used to adjust the level of stimulation applied during the next attempt. Ideally, as the number of repetitions of the task increases, the error between the supplied reference and the measured output position decreases under some appropriate measure. The control system structure exactly corresponds with that of ILC for engineering applications, with a background on this control design method provided in "ILC Basics." Over the course of several treatment sessions, in which a variety of tasks are trained, the voluntary effort supplied by the patient should increase and the level of stimulation assistance decrease. The ultimate aim is that the patient relearns how to do the movement without any added stimulation.

A stroke patient ideally needs to relearn complex functional 3-D tasks but there are many two-dimensional (2-D) tasks where rehabilitation would also significantly improve mobility. The latter are considered in this section and a robotic-based rehabilitation system is described from design through to clinical trial results [33]–[35], [39]–[41], given in the next section, where model-based ILC is used to control the level of FES applied.

Stroke patients typically exhibit partial paralysis on one side of the body and, as a result, have little or no ability to reach out with the affected arm in the 2-D plane, for example, to an object across a flat table top. In the robotic-assisted system of [33]–[35], [39]–[41] patients are seated with their arm supported by the robot and elliptical reaching trajectories are projected onto a target above their hand. FES is then applied to their tricep muscle to assist their tracking of a point that moves along the reference trajectory. At the end of the task, the arm is returned to the starting position in preparation for the next trial. During the reset time, plus a rest time to prevent muscle fatigue, an ILC algorithm is used to calculate the stimulation to be applied on the subsequent trial. The aim is that, as the number of trials increases, the error between the illuminated spot traveling along the reference trajectory and the actual path followed by the patient's hand goes to zero. Figure 1 shows a frontal view of a patient using the system, and Figure 2 shows a plan view, showing the position of the patient's arm and the reference trajectory to be followed with the hand supported by the robot. Figure 3 is a schematic of the robotic workstation and shows the signal flow.

In Figure 1, surface electrodes that deliver the FES to assist the tracking task are shown located on the patient's triceps. The choice of this muscle is based on clinical need since patients typically have difficulty with arm extension. The controlled input variable is the pulsewidth of the applied stimulation. The workstation employs the robotic arm to constrain the arm to move in the horizontal plane, to recreate the effect that the subject is moving a simple point

ILC Basics

An often-encountered industrial control application involves a system or machine that repeatedly performs the same task, at the end of which resetting to the starting location occurs prior to the task being repeated. An example is a gantry robot undertaking a pick and place operation where the following steps must be undertaken in synchronization with a conveyor system: collect an object from a fixed location, transfer it over a fixed, finite duration, place it on a moving conveyor, return to the original location for the next object, and then repeat the previous four actions for as many objects as required.

A controller with no learning applied will give the same tracking error on each trial and although outputs, inputs, and error signals from previous trials are available and rich in information, they are not used by a controller with no learning capability. The objective of iterative learning control (ILC) [S1] is to improve the performance from trial-to-trial by using previous trial information in the construction of the current trial input. ILC differs from other learning-type control paradigms, such as adaptive control, in modifying the control input rather than the controller. Controllers designed in the ILC setting can achieve a high performance with low transient tracking error even in the presence of large model uncertainty and repeating disturbances.

Let $u_k(t)$ denote the input to the system on trial k which is of duration T, that is, $0 \le t \le T < \infty$ and let $r(t)$ denote the desired or reference signal, which does not depend on the trial number. The error on trial k is

$$e_k(t) = r(t) - y_k(t) \tag{S1}$$

and the objective of constructing a sequence of input functions such that the performance achieved is gradually improved with each successive trial can be refined to a convergence condition on the input and error, that is,

$$\lim_{k \to \infty} \|e_k\| = 0, \ \lim_{k \to \infty} \|u_k - u_\infty\| = 0, \tag{S2}$$

where $\|\cdot\|$ denotes the norm on the underlying function space. In this formulation, u_∞ is termed the learned control.

ILC is an established area in control systems research [S2], [S3], in both the underlying theory, experimental verification, and application to physical systems. The ILC algorithms currently available include those with a simple structure that do not require an explicit plant model, such as the P-type ILC. Consider an application operating in discrete time where the noise present is such that deterministic signals can be assumed. Then P-type ILC has the form

$$u_{k+1}(t) = u_k(t) + \Gamma e_k(t), \tag{S3}$$

where Γ is the proportional learning gain that could be allowed to vary form trial-to-trial. At the start of each new trial the complete previous trial output is available and, hence, it is also possible to utilize the error at advanced time steps. One example is phase-lead ILC, which takes the form

$$u_{k+1}(t) = u_k(t) + \Gamma e_k(t + \lambda). \tag{S4}$$

How to fully exploit the use of previous trial data is one of the major questions to be answered in both theory and application domains. A review of the ILC literature demonstrates that simple structure algorithms such as the P-type can be highly successful with many experimental implementations reported. Note that ILC is often combined with standard feedback controllers, to achieve baseline tracking and performance.

P-type ILC and phase-lead ILC are special cases of the following law expressed in terms of the z-transform

$$v_{k+1}(z) = v_k(z) + L(z)e_k(z), \tag{S5}$$

where $L(z)$ is a suitable noncausal operator. A wealth of convergence and robustness analysis exists for such a class of update algorithm [S2], [S3]. The form (S5) is also commonly used for nonlinear system models, where $L(z)$ is typically calculated using a time-varying linearized plant description. One example is the Newton method based ILC that is applied in this article.

Linear model based ILC schemes are often based on minimizing a suitable cost function where the available state-space model is often written as

$$x_{k+1}(t + 1) = A(t)x_{k+1}(t) + B(t)u_{k+1}(t),$$
$$y_{k+1}(t) = C(t)x_{k+1}(t), \tag{S6}$$

where $x_k(t)$ is the state vector on trial k. The cost function in norm optimal ILC is

$$J_{k+1}(u_{k+1}) = \frac{1}{2} \sum_{t=0}^{T} \left(e_{k+1}^T(t) Q e_{k+1}(t) \right.$$
$$\left. + \left(u_{k+1}(t) - u_k(t)\right)^T R \left(u_{k+1}(t) - u_k(t)\right) \right), \tag{S7}$$

where Q and R are symmetric positive definite matrices.

The cost function (S7) is the ILC version of the linear quadratic performance criterion from optimal control theory and is a combination of the optimal tracking of the reference and the disturbance accommodation, regarding $u_k(t)$ as a known disturbance on trial $k + 1$. The term $u_{k+1}(t) - u_k(t)$ is the difference in the control input on successive trials and this algorithm aims for optimal reduction of the current trial error without an excessive change in the control input used on the previous trial.

The norm optimal ILC solution computes the current trial control input as

$$u_{k+1}(t) = u_k(t) - \{B^T(t)K(t)B(t) + R\}^{-1} B^T(t)K(t)A(t)\{x_{k+1}(t)$$
$$- x_k(t)\} + R^{-1}B^T(t)\xi_{k+1}(t), \tag{S8}$$

where

$$\xi_{k+1}(t) = \{I + K(t)B(t)R^{-1}B^T(t)\}^{-1}\{A^T(t)\xi_{k+1}(t+1)$$
$$+ C^T(t)Qe_k(t+1)\}, \quad \xi_{k+1}(T) = 0 \qquad (S9)$$

and

$$K(t) = A^T(t)K(t+1)A(t) + C^T(t)QC(t) - A^T(t)K(t+1)B(t)$$
$$\times \{B^T(t)K(t+1)B(t) + R\}^{-1}B^T(t)K(t+1)A(t), \, K(T) = 0. \qquad (S10)$$

The Ricatti equation (S10) need only be solved once before the trials begin and the predictive component (S9) can be computed in the resetting time between successive trials [S4].

Of the currently available ILC algorithms for nonlinear dynamics, this article makes use of the Newton ILC where the control update is

$$u_{k+1} = u_k + g'(u_k)^{-1}e_k,$$

where $g'(u_k)$ is the system Jacobian. Calculating the inverse is computationally expensive and may lead to ill conditioning, but rewriting the last equation as

$$u_{k+1} = u_k + z_{k+1},$$

corresponds to solving the equation

$$z_{k+1} = g'(u_k)^{-1}e_k,$$

or

$$e_k = g'(u_k)z_{k+1}.$$

This avoids calculation of the inverse and can be solved by any ILC algorithm that results in global convergence for an arbitrary LTV system, such as norm optimal ILC [S4].

REFERENCES
[S1] S. Arimoto, S. Kawamura, and F. Miyazaki, "Bettering operations of robots by learning," J. Robot. Syst., vol. 1, pp. 123–140, 1984. **<AU: Kindly provide the issue no.>**
[S2] D. A. Bristow, M. Tharayil, and A. G. Alleyne, "A survey of iterative learning control," IEEE Contr. Syst. Mag., vol. 26, no. 3, pp. 96–114, 2006.
[S3] H.-S. Ahn, Y. Chen, and K. L. Moore, "Iterative learning control: Brief survey and categorization," IEEE Trans. Syst., Man, Cybern. C, vol. 37, no. 6, pp. 1109–1121, 2007.
[S4] N. Amann, D. H. Owens, and E. Rogers, "Iterative learning control using optimal feedback and feedforward actions," Int. J. Control, vol. 65, no. 2, pp. 277–293, 1996.
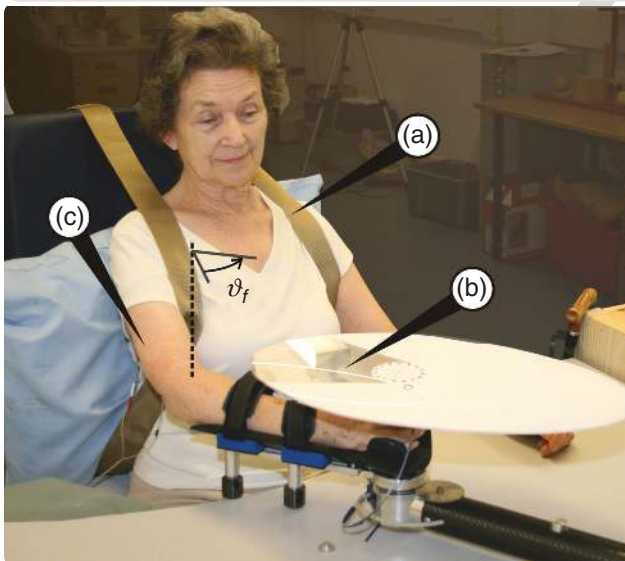
FIGURE 1 A frontal view of a patient using the planar robotic workstation showing (a) shoulder strapping, (b) tracking task, and (c) surface electrodes. The patient is seated with her arm supported by the robot and elliptical trajectories are projected onto a target above the hand and functional electrical stimulation is applied to her triceps, using the surface electrodes, in order to assist tracking of a point that moves along the reference trajectory. At the end of the task, the arm is returned to the starting position in preparation for the next trial. During the reset time, plus a rest time to prevent muscle fatigue and allow transients to decay, an iterative learning control algorithm is used to calculate the stimulation to be applied on the subsequent trial. The stimulation applied to the triceps muscle produces a torque about the elbow and the control problem is equivalent to controlling the angle ϑ_f. The shoulder strapping is to prevent forward movement by the patient's trunk during the trials, which would conflict with the desired objective of reaching out with the arm.

mass with damping, and to provide assistance about the shoulder since the FES applied is unable to actuate this joint. The emphasis, however, is on FES driving the task completion rather than the robot. The strapping shown in
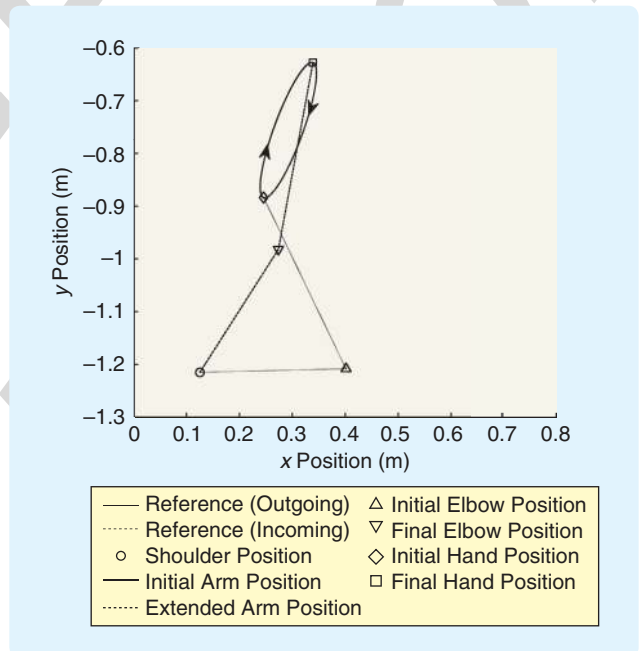

FIGURE 2 An example of the tracking task geometry for a patient with right-hand-side hemiplegia for the planar case, showing the initial and final positions of the elbow, shoulder, and arm, respectively. The iterative learning control adjusted stimulation is applied during the time when the outgoing reference is the target to be achieved.
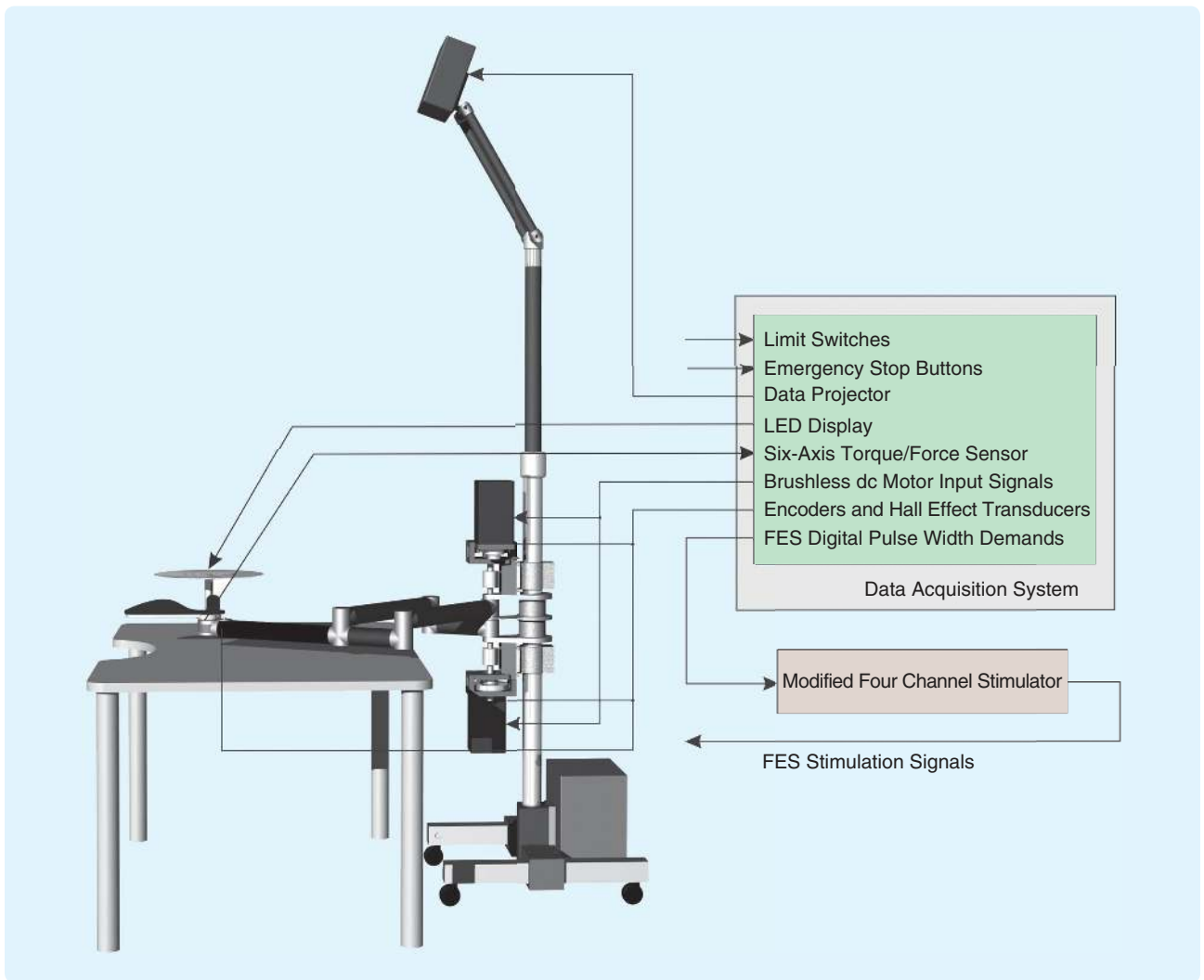
FIGURE 3 Schematic of the robotic workstation. The data flow, and how the various signals required are physically measured and applied, are highlighted. The limit switches and emergency stop buttons are required in order to obtain ethical clearance for experiments with human subjects.

Figure 1 is to prevent forward movement by the patient's trunk during the trials, which would conflict with the desired objective of reaching out with the arm. In control systems terms, it is the forearm angle $\vartheta_f(t)$ that forms the controlled variable, which is required to track a supplied reference $\vartheta_f^*(t)$.

Figure 4 shows a block diagram of the control scheme used in the clinical trials, consisting of a feedback controller, a linearizing controller, and an ILC feedforward controller. The former block acts as a prestabilizer and provides satisfactory tracking during initial trials. During the arm resetting time at the end of trial k, the ILC controller uses a biomechanical model of the arm and muscle system, along with the previous tracking error, to calculate the feedforward update signal $v_{k+1}(t)$ for application on the next trial. To explain the presence of the feedback controller, a large class of ILC algorithms for discrete linear systems is based on lifting the dynamics into an equivalent standard linear

system state-space model that describes the trial-to-trial updating. If the system considered is unstable or has unacceptable transient dynamics, a feedback loop is first designed to stabilize or suitably control the response, and ILC is applied to the resulting controlled dynamics.

The accuracy of the human arm and muscle model has a strong effect on the overall performance of the control scheme of Figure 4, and is constructed from a stimulated muscle structure that accounts for the torque $y(t)$ acting about the elbow generated in response to the applied FES $u(t)$, and a two-link system that produces the resulting angular movement $\vartheta_f(t)$. The biomechanical model employed during the clinical trials is specifically developed for stroke patients [33] and is identified by kinematically exciting the arm and optimally fitting parameters using a least-squares criterion.
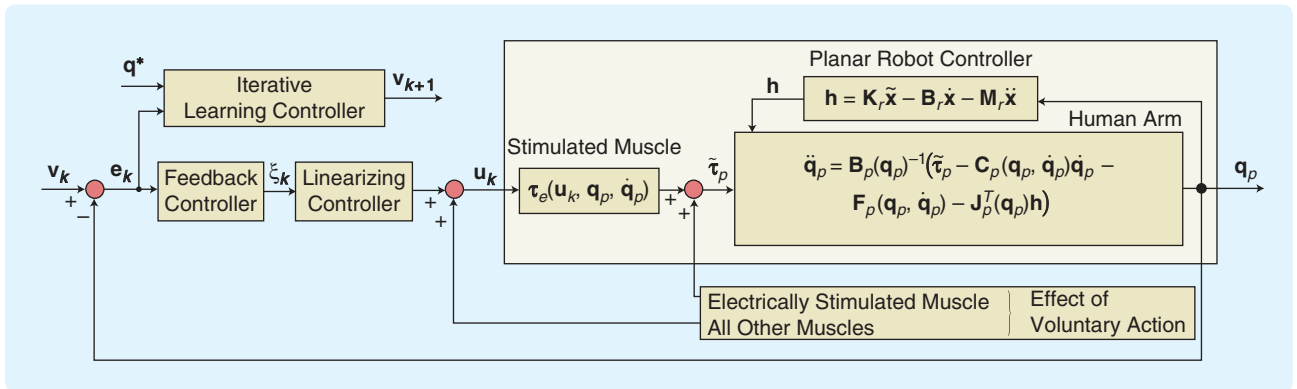
FIGURE 4 Block diagram representation of the iterative learning control (ILC) scheme in the planar case, consisting of a feedback controller, a linearizing controller, and an ILC feedforward controller. The former block, taken as a proportional plus derivative controller, acts as a prestabilizer and provides satisfactory tracking during initial trials. During the arm resetting time at the end of trial k, the ILC controller uses a biomechanical model of the arm and muscle system, along with the previous tracking error, to produce the feedforward update signal $v_{k+1}(t)$ for application on the next trial.

FES and the Muscle Model

FES employs short electrical pulses to generate contractions in the muscles that can be coordinated to actuate joints. The intention of FES is often orthotic, for example, when applied to enable the standing of subjects with complete SCI. More commonly, especially with systems where stimulation is applied through skin surface electrodes, the objective is to achieve a therapeutic response, that is, a functional movement that after repetition leads to improved motor control when the stimulation is not applied. A coverage of FES with particular emphasis on its use in both open and closed-loop control schemes for other biomedical and rehabilitation problems is given in [27].

The lack of closed-loop model-based strategies in FES technology, especially for the upper limb, is primarily due to the difficulty in obtaining an accurate plant model. Muscle models form a crucial part of such a representation, and vary widely in structure in the model-based controllers reported in the literature. No explicit form of muscle model is used in [42]–[44], linear forms are employed in [22], [45] and a general nonlinear form is given in [21]. The

most widely assumed structure is the Hill-type model [46], which describes the output force as the product of three independent experimentally measured factors, that is, the force-length property, the force-velocity property, and the nonlinear muscle activation dynamics under isometric conditions, respectively.

The form of the first two experimentally measured factors is chosen to correspond with physiological observations [47]–[49]. The activation dynamics (AD) are almost always represented by a static nonlinearity in series with linear dynamics, and constitute an important component of the model since controlled motions are typically smooth and slow; therefore the effects of inertia, velocity, and series elasticity are small, and the isometric behavior of muscle dominates. The nonlinearity is parameterized in several ways, taking the form of a simple gain with saturation in [50], a piecewise linear function [47], [51], and a predefined functional form in [52] and [53]. The linear dynamics are assumed to be first order in [47], a series of two first-order systems in [48], [54], critically damped second order in [55]–[57], and second-order system with a possible transport delay in [58] and [51].

The use of Hammerstein structure representations of the activation dynamics is supported by a correspondence with biophysics where the static nonlinearity, denoted $h_{IRC}(u)$, represents the isometric recruitment curve (IRC) which is the static gain relation between stimulus activation level $u(t)$ and steady-state output torque $w(t)$ with the muscle held at a fixed length. The linear activation dynamics (LAD) represents the muscle contraction dynamics $h_{LAD}(s)$, with s denoting the Laplace transform variable, which convolve with the IRC to give the overall torque generated $y(t)$. The block diagram representation of this muscle representation is given in Figure 5 with expanded discussion in "Modeling Human Muscle Response to FES Stimulation."
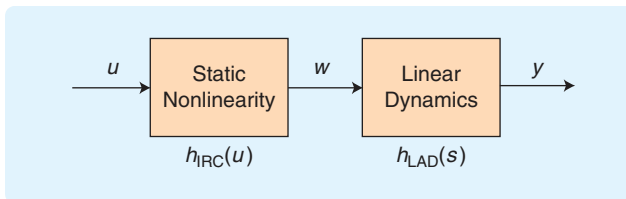

FIGURE 5 Hammerstein structure representation of activation dynamics. The static nonlinearity, denoted by $h_{IRC}(u)$, represents the isometric recruitment curve, that is, the static gain relation between stimulus activation level $u(t)$ and steady-state output torque $w(t)$, when the muscle is held at a fixed length. The linear activation dynamics represents the muscle contraction dynamics $h_{LAD}(s)$, which convolve with the isometric recruitment curve to give the overall isometric torque generated, denoted $y(t)$, about the elbow.

Modeling Human Muscle Response to FES Stimulation

Three limitations restrict the application of the Hammerstein structure [S5] to upper-limb stroke rehabilitation and must be overcome. The first limitation is that functional electrical stimulation (FES) is applied to either in vitro or paretic muscles in the vast majority of experimental verification tests, thus removing the possibility of an involuntary response to stimulation that may occur when applied to subjects with incomplete paralysis, such as stroke. In addition to motivating the need for experimental validation on such subjects, the excitation inputs used widely to identify the Hammerstein structure, that is, pseudo-random-binary sequences (PRBS) white noise, and pulses, are not appropriate since they would elicit an involuntary response from the subject.

The second restriction is the absence of test results from subjects with incomplete paraplegia, which means that physiologically based constraints on the form of the dynamics, such as the assumption of a critically damped system [S6], [S7], may not be justified. Thirdly, almost all previously reported in vivo studies and control implementations have applied FES to the lower limb, even though upper-limb functional tasks require finer control, and are more subject to adverse effects such as sliding electrodes and the activation of adjacent muscles during stimulation.

To address such drawbacks, identification schemes and accompanying sets of excitation inputs are developed in [S5]. The excitation signal must be chosen from a physiological perspective, and hence the identification scheme cannot use rapidly changing inputs and must be applicable to an arbitrary choice of signal. Moreover, a general form of linear dynamics represented in transfer-function form is used, together with a smooth function with continuous derivatives in the representation of the static nonlinearity since it is preferable to that of a piecewise linear function. Detailed investigation in [S5] led to four candidate tests for use in the identification of electrically stimulated muscles in stroke patients and examples of the excitation inputs employed in each are given in Figure S1.

Experimental tests to identify and validate muscle models are performed using the iterative learning control (ILC) workstation so that conditions and setup procedures match exactly those used in clinical trials. During the experiments, the position of the robotic arm is fixed using a locking pin, at an elbow extension angle of approximately $\pi/2$ rad. This removes the nonisometric components of the biomechanical model, and the resulting system corresponds to the Hammerstein structure shown in Figure 5. Detailed comparison of the algorithms and excitation inputs can be found in [S5], where greatest performance levels are observed using the staircase test input that avoids the problem of eliciting a voluntary response, whilst still proving sufficiently exciting. Although these algorithms provide high levels of performance and are suitable for stroke rehabilitation, they are only valid in short time intervals due to the slowly time-varying properties of the muscle system caused by fatigue, spasticity, and other physiological effects. Motivated by such deficiencies, recursive versions of the procedures are developed in [S8] that are suitable for the conditions encountered during clinical trials. The development and analysis of ILC algorithms using such recursively updated plant models is an open research problem.

REFERENCES

[S5] F. Le, I. Markovsky, C. T. Freeman, and E. Rogers, "Identification of electrically stimulated muscle models of stroke patients," Control Eng. Pract., vol. 18, no. 4, pp. 396–407, 2010.
[S6] L. Bernotas, P. E. Crago, and H. J. Chizeck, "A discrete-time model of electrically stimulated muscle," IEEE Trans. Bio-Med. Eng., vol. 33, no. 9, pp. 829–838, 1986.
[S7] W. K. Durfee and K. I. Palmer, "Estimation of force-activation, force-length, and force-velocity properties in isolated, electrically stimulated muscle," IEEE Trans. Bio-Med. Eng., vol. 41, no. 3, pp. 205–216, 1994.
[S8] F. Le, I. Markovsky, C. T. Freeman, and E. Rogers, "Recursive identification of Hammerstein systems," in Proc. 18th IFAC World Congr., Milan, Italy, 2011, pp. 13954–13959.

Planar Arm Model

Figure 6 shows the geometry of the dual human and robotic system, in which x_0, y_0, and z_0 are components of the robotic base coordinate frame, and x, y, and z are those of the human arm base coordinate frame, with the two systems related by a translation. The robot joint angle vector is $q_r = [\vartheta_1, \vartheta_2]^T$, and the torque supplied by the motor is given by $\tau_r = [\tau_1, \tau_2]^T$, whose components are in the directions of ϑ_1 and ϑ_2, respectively. The upper link of the human arm extends from the acromion to the olecranon process of the elbow, with length l_u. The second link represents the forearm, from the elbow to the thumb web, with length l_f.

The constraint imposed by connecting the hand to the robot requires the forearm to lie in the horizontal plane and rotation is possible about the axis along the upper arm. Assistance is provided by the triceps, modeled as supplying a torque $\tau_e \geq 0$ acting about an axis orthogonal to both the upper arm and forearm. The subject interacts with the robot by applying a vector of forces and torques at the point Q, which has a z_0 component of l_z. The vector of the components of the forces applied in the x and y directions, respectively, is given by $h_r = [F_x, F_y]^T$. A form of impedance control is used to govern the torque demand supplied to the motors in order to guarantee safe interaction with patients [59]. The resulting relationship is given by

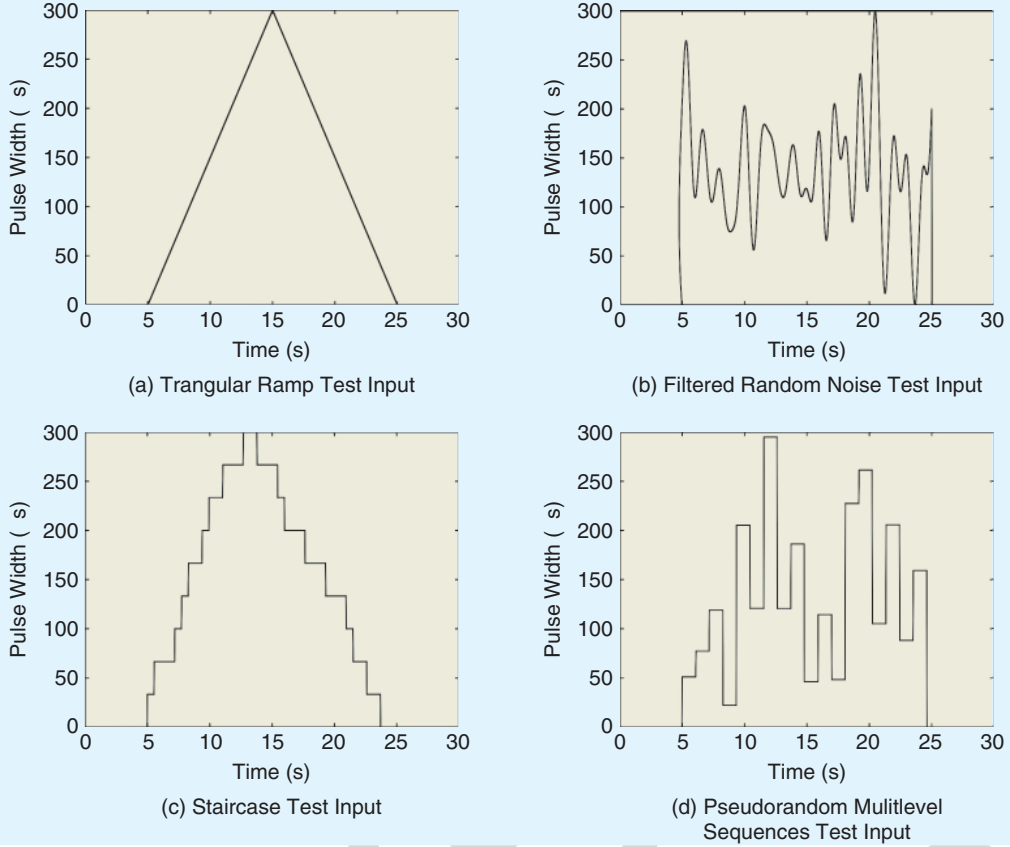$$-h_r = K_r \tilde{x} - B_r \dot{x} - M_r \ddot{x}, \tag{1}$$

FIGURE S1 An example of four candidate tests. In the triangular ramp test of (a) the pulse duration rises linearly from 0 to 300 μs and then returns to 0, with a uniformly distributed range. In the filtered random noise test of (b), the pulse width signal is produced by low-pass filtering white noise, using a suitable cut-off frequency to balance the opposing physiological and identification issues. Having filtered the signal, an offset and gain are applied to ensure the desired pulsewidth range is spanned. In the staircase test of (c) the duration of each pulse changes step by step. The number of steps should be large enough to identify the nonlinearity and their width chosen carefully. Let $\tau = E_s/4$, where E_s is the 98% settling time, where it is recommended to use mixed step widths, with step width τ for 1/3 of the test period, 2τ for another 1/3 of the test period, 3τ for the remaining 1/3 of the test period, and to randomize widths when creating the test signals. In the pseudo random multi-level sequence test of (d), the excitation signal is an multi-level pseudo random sequence that is a periodic deterministic signal with an autocorrelation function similar to white noise. The amplitude level is uniformly distributed over the full range.

where $\hat{x}$ is the reference position, $\tilde{x} = \hat{x} - x$, $x = k_r(q_r)$, $\dot{x} = J_r(q_r)\dot{q}_r$, and $\ddot{x} = J_r(q_r)\ddot{q}_r + \dot{J}_r(q_r, \dot{q}_r)\dot{q}_r$. Here $x = k_r(q_r)$ is the direct kinematics equation, and $J_r^T(q_r)$ is the system Jacobian. When the robot is moved by the subject with no assistance, the gain matrices have the respective form $K_r = 0$, $B_r = \overline{B}_r I$, and $M_r = \overline{M}_r I$, where $\overline{B}_r$ and $\overline{M}_r$ are positive scalars, to replicate a natural movement task. When the robot is required to move the subject's arm along predefined trajectories, it is necessary to set $K_r = \overline{K}_r I$, with the scalar $\overline{K}_r > 0$ and I denotes the identity matrix with compatible dimensions.

To satisfy the horizontal constraint the elbow angle, that is, the angle between the upper arm and forearm must satisfy

$$\vartheta_e(\vartheta_f) = \arccos(-c_f c_{\bar{\gamma}}), \qquad (2)$$

where $\bar{\gamma}$ denotes the fixed upper arm elevation angle, and c_f and $c_{\bar{\gamma}}$ denote $\cos(\vartheta_f)$ and $\cos(\bar{\gamma})$, respectively, and like-

wise for $\sin(\cdot)$. The dynamic model of the constrained arm can now be expressed in the form

$$B_p(q_p)\ddot{q}_p + C_p(q_p, \dot{q}_p)\dot{q}_p + F_p(q_p, \dot{q}_p) = \tau_p - J_p^T(q_p)h, \qquad (3)$$

where $B_p, C_p \in \mathcal{R}^{2 \times 2}$ are the inertial and Coriolis matrices, respectively, as detailed for the planar system in [34], $q_p = [\vartheta_u, \vartheta_f]^T$ is the joint angle vector, $J_p(q_p)$ is the system Jacobian and the external force vector satisfies $h = h_r$ as a consequence of the connection with the robotic arm. The moment vector about the forearm axis produced by applied FES is

$$\tau_p = \begin{bmatrix} 0 \\ \tau_e \sigma(\vartheta_f) \end{bmatrix}, \quad \sigma(\vartheta_f) = \frac{-s_f c_{\bar{\gamma}}}{\sqrt{1 - c_f^2 c_{\bar{\gamma}}^2}}. \qquad (4)$$

The decoupled form of the nonconservative force $F_p(q_p, \dot{q}_p) = [F_u(\vartheta_u, \dot{\vartheta}_u), F_f(\vartheta_f, \dot{\vartheta}_f)]^T$ provides a satisfactory compromise between repeatability and the accuracy of the overall model [33] and includes effects such as spasticity.
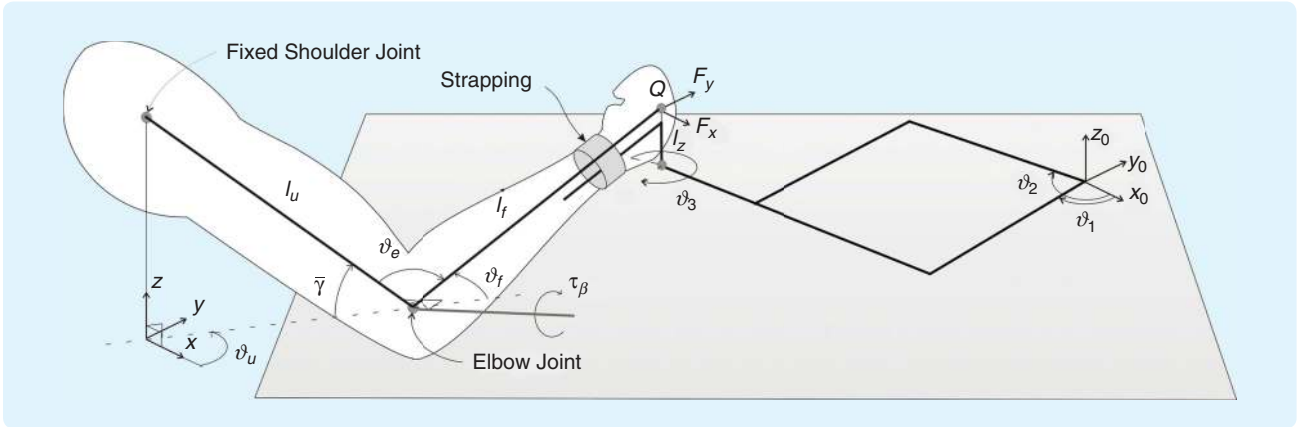
FIGURE 6 Geometry of dual planar human arm and robotic system. In the notation used, x_0, y_0, and z_0 are components of the robotic base coordinate frame, and x, y, and z are those of the human arm base coordinate frame, and the two systems are related by a translation. The robot joint angle vector is $q_r = [\vartheta_1 \ \vartheta_2]^T$, and the torque supplied by the motor is $\tau_r = [\tau_1 \ \tau_2]^T$, whose components are in the directions of ϑ_1 and ϑ_2, respectively. The upper link of the human arm extends from the acromion to the olecranon process of the elbow, with length l_u. The second link represents the forearm, from the elbow to the thumb web, with length l_f.

The torque, τ_e, generated by electrically stimulated muscle acting about a single joint is given by

$$\tau_e(u, \vartheta_e, \dot\vartheta_e) = h(u, t) \times F_m(\vartheta_e, \dot\vartheta_e) + F_s(\vartheta_e, \dot\vartheta_e), \qquad (5)$$

where the term $h(u, t)$ represents the Hammerstein structure shown in Figure 5. The term $F_m(\vartheta_e, \dot\vartheta_e)$ models the multiplicative effect of the joint angle, and joint angular velocity, respectively, on the active torque developed by the muscle [33]. The term $F_s(\vartheta_e, \dot\vartheta_e)$ accounts for the passive properties of the joint. Since $\bar\gamma$ is invariant, (2) means that $F_s(\vartheta_e, \dot\vartheta_e)$ is accounted for when the general form $F_f(\vartheta_f, \dot\vartheta_f)$ is used and can therefore be omitted. The FES drives completion of the task by assisting movement about the elbow, the robotic arm is purely only of assistance about the shoulder. To provide assistance torque solely about the upper-arm axis to follow a reference $\hat\vartheta_u$, (3) gives that a suitable form of the robotic control force (1) is

$$h = J_p^{-T}(q_p) \begin{bmatrix} K_u(\hat\vartheta_u - \vartheta_u) - B_u\dot\vartheta_u - M_u\ddot\vartheta_u \\ -B_f\dot\vartheta_f - M_f\ddot\vartheta_f \end{bmatrix}, \qquad (6)$$

with parameters $\{K_u, B_u, M_u\}$ and $\{B_f, M_f\}$ governing the dynamic components about the upper arm and forearm, respectively. The form (6) is achieved through appropriate selection of K_r, B_r, and M_r in the robotic arm (1). It is shown in [34] that the parameter $\hat{x}$ is the point of intersection of the reference path and a line extending along the forearm, which confirms that tracking assistance is applied only about the upper arm. If $\hat\vartheta_u$ is chosen to be sufficiently smooth, the upper arm dynamics are decoupled from the system (3) to leave only the forearm dynamics, shown in Figure 7, which are used for FES control law design [34].

Planar Control Schemes

The strategy selected to control the stimulation applied to the subject consists of a linearizing controller in a feedback arrangement, with an additive ILC feedforward controller as shown in Figure 4. This representation includes a model
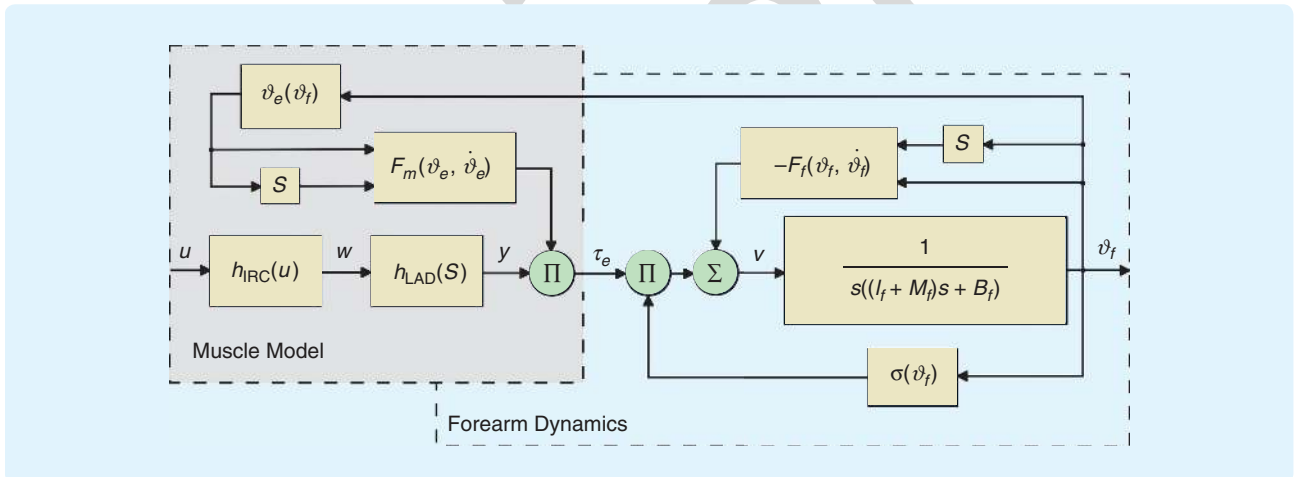

FIGURE 7 Continuous-time model of stimulated planar human arm used in control law design for planar case.

of the influence of the patient's volitional action. Although this can be captured by the recording of EMG during movement, the incorporation of EMG into model-based controllers is only beginning to receive attention in the literature, but is not well understood [60]. Within the ILC framework the trial-invariant component of voluntary effort can be treated as a repeating disturbance and completely canceled, however incorporation of EMG within the model is still an open problem. The first component of the linearizing controller is the inverse of the isometric recruitment function identified for each subject. The controller's subsequent action is motivated by the form of the remaining nonlinear terms $\sigma(\vartheta_f)$, $E_f(\vartheta_f, \dot{\vartheta}_f)$, and $E_m(\vartheta_e, \dot{\vartheta}_e)$, respectively, in the arm model of Figure 7. All three functions vary slowly when the trajectories used for rehabilitation are followed with an error that is small in magnitude, and consequently the control action employed comprises a steady-state linearization approach to remove their effect, creating a system that approximates the linear activation dynamics in series with the linear arm dynamics [33]. The approximate linearizing controller, with input ξ, is given by

$$u = h_{IRC}^{-1}\left(\frac{E_f(\vartheta_f, \dot{\vartheta}_f) + \xi}{\sigma(\vartheta_f) E_m(\vartheta_e, \dot{\vartheta}_e)} \right), \qquad (7)$$

and in combination with the robotic controller produces

$$\frac{\vartheta_f(s)}{\xi(s)} = h_{LAD}(s)\frac{1}{s((I_f + M_f)s + B_f)} = G(s), \qquad (8)$$

where I_f is the inertia of the forearm with respect to the elbow. Results and analysis given in [34] confirm that (8) accurately approximates the combined approximate linearizing controller and arm system for the range of trajectories and arm dynamics required in stroke rehabilitation. A limitation of the controller (7) is that the system (8) is not an accurate representation at high frequencies but this is not a major problem at the initial feasibility phase of research in this problem area.

To supply the torque demand ξ, a proportional derivative (PD) controller $C(s)$ is tuned individually for each subject. The resulting bandwidth is limited in the main by the stipulated end-effector dynamics and the muscle dynamics. Many ILC algorithms have been developed and experimentally tested in engineering applications, but with the aim of keeping the overall scheme as simple as possible in the initial feasibility phase attention is restricted to two simple structure algorithms.

The phase-lead ILC algorithm can provide high performance, despite its simplicity and limited parameter set, and is given in z-transform terms by

$$v_{k+1}(z) = v_k(z) + Lz^\lambda e_k(z), \qquad (9)$$

where the error is calculated as $e_k(t) = \vartheta_f^*(t) - \vartheta_{f,k}(t)$, L is a scalar gain, λ is the phase-lead in samples, k is the trial number, and v_{k+1} is the updated control input. The controller is selected based on the nominal system $P(z) = (C(z)G(z))/(1 + C(z)G(z))$ and then tuned heuristically. Higher frequencies that may gradually increase are removed by a noncausal zero-phase filter applied to either the error or control input v_{k+1} [61], however the small number of trials undertaken means that this is unnecessary in the present application. The sampling time is $(1/40)$-s in correspondence with the frequency at which the stimulation pulses are applied to the patient.

The adjoint ILC algorithm is an alternative to (9) with z-transform representation

$$v_{k+1}(z) = v_k(z) + KP^*(z)e_k(z), \qquad (10)$$

where $(\cdot)^*(z)$ denotes the noncausal adjoint operator. An added feature of this controller is that, when applied to the nominal plant $P(z)$ with a sufficiently small scalar multiplier, K, it is guaranteed to satisfy the condition for monotonic convergence over all frequencies, and hence ensure a satisfactory transient response.

Experimental Results with Unimpaired Subjects

The ILC algorithms (9) and (10) were implemented on ten unimpaired subjects taking part in a preliminary study. This study established the efficiency of control schemes prior to ethical approval and their subsequent use in a clinical trial with stroke patients. For each subject the isometric muscle model was first identified using tests described in "Modeling Human Muscle Response to FES Stimulation," and then components of the arm model dynamics (3) were identified through injection of sufficiently rich kinematic trajectories by the robot and least mean fitting of the resulting kinematic and force data [33]. The reference trajectories mimicked natural reaching movements for the impaired arm and Figure 2 shows an example of the reference path used in relation to the position of the subject's glenohumeral joint. In this case the reference is set at an angle of $20°$ from the y axis, and individually calculated for each subject to extend their arm from 55% to 95% of their total arm length over the course of the movement.

By moving along the extension half of this reference at two speeds, two trajectories are created. For validation on unimpaired subjects only the first outgoing half of the reference is used. Each trajectory starts with a waiting period where its value is set equal to the starting point of the reference. The slow trajectory lasted for 12.5 s in total, composed of a 5-s waiting period and a 7.5-s movement along the reference, and the fast trajectory lasts for 10 s, composed of a 5-s waiting period followed by a 5-s movement. The waiting period allows the ILC update to begin before the arm is required to move. Before each trial commences, the subject's arm is moved to the initial posi-
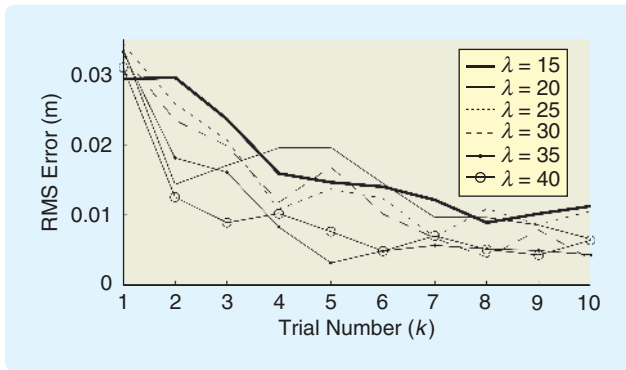
FIGURE 8 Single unimpaired subject experimental results using the phase-lead iterative learning control law (9). Results for various values of λ are given for the slow trajectory together with proportional derivative controller gains of $K_p = 10$ and $K_d = 2$. The learning gain in the control law (9) is chosen as $L = 0.2$, and consequently the speed of convergence is traded-off for greater robustness. The root mean square (RMS) corresponding to this phase-lead converges to approximately 5 mm and has a minimum value of 3.2 mm.

tion by the robot and released only when the trajectory starts. The subjects are not shown the trajectory before or during the test.

The values of B_f and M_f that dictate the end-effector characteristic are set at 5.78 Nm/rads^{-1} and 0.29 Nm/rads^{-2}, respectively, creating a natural feel to the system and allowing the chosen trajectories to be completed with moderate effort without limiting the bandwidth excessively. The feedback controller gains are tuned for each subject with emphasis on robustness rather than performance.

Figure 8 gives representative results for a single subject using the phase-lead ILC algorithm (9) for various values of λ. The slow trajectory is used together with PD controller gains of $K_p = 10$ and $K_d = 2$. The learning gain in (9) is chosen conservatively as $L = 0.2$, and therefore the speed of convergence is sacrificed for greater robustness. The root mean square (RMS) error corresponding to this phase-lead controller converges to approximately 5 mm with a minimum value of 3.2 mm. Figure 9 shows the results obtained using $L = 0.2$ and $\lambda = 35$ in greater detail, where during the first five trials the error reduces monotonically and the reference is closely tracked. The effect of the linearizing feedback controller in the absence of ILC is seen by inspection of the first trial with the ILC action applied.

Figure 10 shows the associated stimulation inputs and ILC updates, where from Figure 10(a) the stimulation applied during $k = 1$ saturates at 300 μs, but that the effect of further trials removes this effect and produces lower levels of stimulation over the course of the trial. Moreover, ILC results in the application of stimulation during the initial 5-s waiting period before movement is required. Figure 10(b) shows that the updated reference v_{k+1} converges to a fixed trajectory over repeated trials.

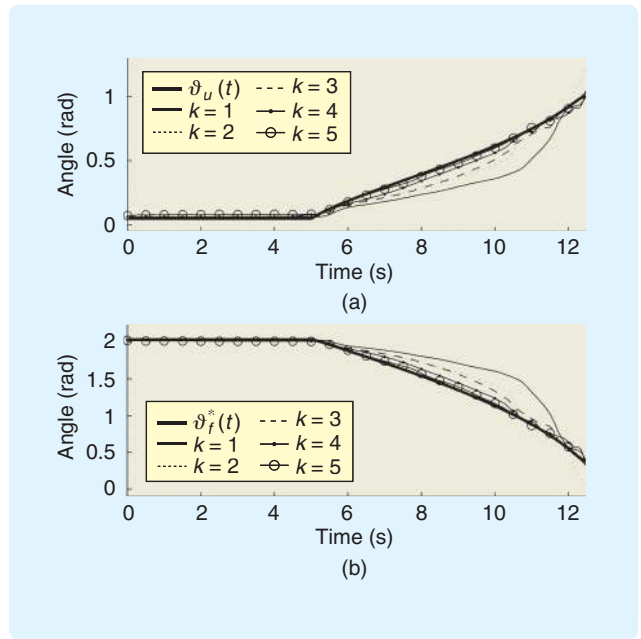Figure 11 gives results from the first four subjects tested in the preliminary study using the adjoint ILC algorithm

FIGURE 9 Single unimpaired subject experimental tracking, where (a) is for $\vartheta_u(t)$, and (b) for $\vartheta_f(t)$, respectively, for the slow trajectory using the phase-lead iterative learning control (ILC) law (9) with $L = 0.2$ and $\lambda = 35$. The effect of the linearizing feedback controller in the absence of ILC is seen by inspection of the first trial results.
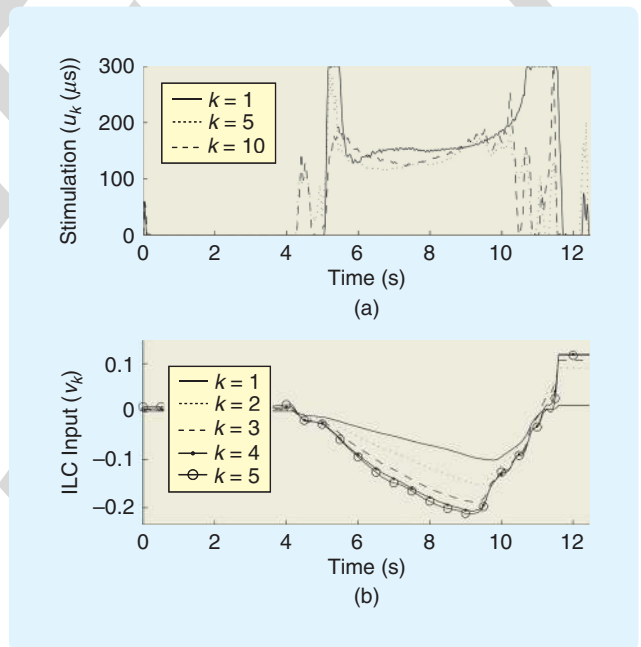

FIGURE 10 Single unimpaired subject experimental results. The results are from the phase-lead iterative learning control (ILC) algorithm (9) with $L = 0.2$ and $\lambda = 35$, and the slow trajectory, and give the stimulation inputs and ILC updates. Part (a) shows that the stimulation applied on the first trial saturates at 300 μs, but that the effect of further trials produces lower levels of stimulation over the course of the trial. Moreover, use of ILC results in the application of stimulation during the initial 5-s waiting period before movement is required. Part (b) shows that the updated reference v_{k+1} is converging to a fixed trajectory over repeated trials.
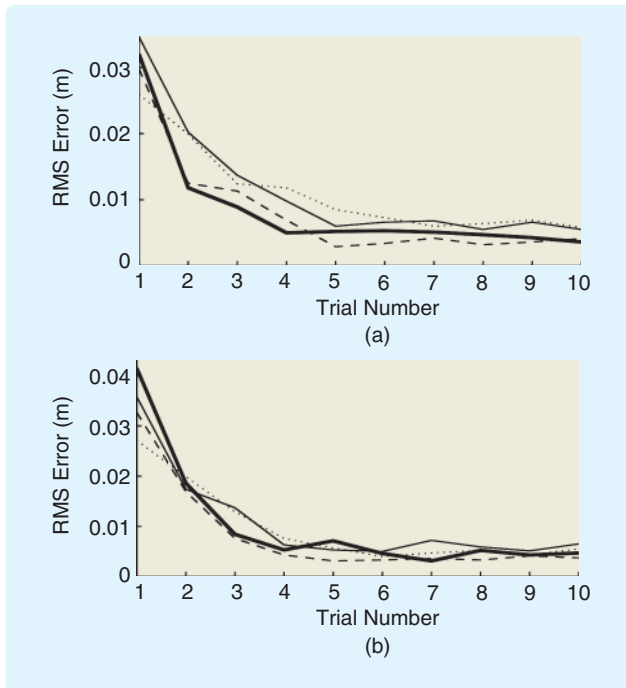
FIGURE 11 Results for the adjoint iterative learning control law (10) applied with four unimpaired subjects with $K = 0.2$. Part (a) is for the slow trajectory, and (b) the fast trajectory. The results demonstrate that convergence can be achieved within five trials for both trajectories, and a root mean square (RMS) tracking error of less than 10 mm over the course of the movement is possible in all cases.

TABLE 1 Mean (standard deviation) of last trial root mean square (RMS) error for all 18 subjects using the planar robot system.

Type	Mean of last trial RMS error /mm	
	20° trajectory	40° trajectory
Slow	9.41 (5.67)	10.22 (6.07)
Fast	12.18 (6.94)	12.93 (6.87)

(10), where the results in Figure 11(a) and (b) are for the slow and fast trajectories, respectively. These results demonstrate that convergence can be achieved within five trials for both trajectories, and an RMS tracking error of less than 10 mm over the course of the movement is possible in all cases. The effect of model uncertainty, unmodeled dynamics, nonrepeatable disturbance, and noise degrades the property of monotonic error convergence. Similar results are obtained using a reference whose inclination is increased from 20° to 40° from the y axis. Table 1 shows the mean and standard deviation of the RMS error obtained during the last trial, for both trajectories and all 18 subjects tested.

These results confirm that the control laws (9) and (10) are capable of producing high levels of tracking accuracy for unimpaired subjects. The next section gives results from a clinical trial with stroke patients and discusses how the results obtained are assessed in this domain.

CLINICAL ASSESSMENT

The ILC algorithms of the previous section were applied during a clinical trial with five stroke patients. The evaluation of any rehabilitation intervention is critical to establish effect, that is, the benefit or otherwise to the patient. Choosing an appropriate clinical outcome measure requires a structured approach to selecting the relevant domains and establishing the criteria to evaluate the measures. The World Health Organization's International Classification of Functioning, Disability, and Health (ICF) which is a framework for measuring both health and disability [62], is helpful in determining suitable outcome measures. This classification consists of domains that are health and health related, described in the form of two lists, body functions and structures, and activity and participation, respectively. Within the classification, impairments are defined as problems in body function or structure (e.g. a significant deviation or loss), activity is the execution of a task or action by an individual, and participation is involvement in a life situation society.

Active assisted or partially facilitated exercises are recommended clinically in the United Kingdom for stroke patients who are unable to move by themselves [63], and to measure the effectiveness of such techniques, physiotherapists are more likely to use activity or participant based outcome measures. Impairment based measures, which normally require more equipment, explain why the changes are seen. In the clinical assessment of the ILC designs of the previous section, both the domains of impairment and activity and relevance to literature, respectively. The forms of reliability considered included internal consistency, whether the test items measure the outcome consistently, and inter-rater reliability. The forms of validity considered are content, that is, whether the assessment items reflect the domain they claim to measure, construct, that is, whether the assessment measures the known attributes of the theoretical construct under evaluation, and criterion validity, that is, the agreement between results of the assessment under evaluation, and a criterion assessment or gold standard. The test time is less than 30 min, due to the number of tests that needed to be performed, and the possibility of stroke participant fatigue. The final general consideration is how widely the test is used either in contemporary rehabilitation robotics, electrical stimulation, or relevant clinical literature. Further background is given in "Clinical Assessment of Stroke Rehabilitation."

Following the University of Southampton ethical approval, five participants, three male and two female, were recruited and gave written consent. Their demographic characteristics are given in [35] and ranged in age

Clinical Assessment of Stroke Rehabilitation

The primary measure chosen for upper limb function is the Action Research Arm Test [S9] (ARAT) developed to monitor function related to everyday tasks and uses a hierarchical measure of grasp, grip, pinch, and gross movement. The reaching and grasping movements are rated on quality and speed in three dimensions. The ARAT assesses primarily activity limitations, that is, a patient's functional loss when interacting with the environment by means of the upper limb. Reliability [S9] and validity are established for the ARAT but the measure shows both floor and ceiling effects, which are limitations for people who have either low or high function. This test is widely used in the electrical stimulation literature.

The primary outcome measure chosen to detect changes in upper limb impairment is the Fugl-Meyer assessment [S10] (FMA). This test primarily assesses impairment in terms of loss or abnormality of movement, that is, the ability to perform movements in accordance with specified joint motion pattern. It provides an adequate, reproducible, and fairly standardized picture of a patient's sensorimotor and joint characteristics. The FMA is an ordinal scale testing gross movement, coordination, and sensation of the upper limb. The test is appropriate for severe to mildly affected patients and has high reliability [S11] and validity [S10]. The widespread use of the FMA in research involving rehabilitation robots [S12], together with its utility and standardized procedure, justify its choice as the impairment outcome measure. In terms of resolution, the FMA could, in contrast to the ARAT, detect differences throughout the spectrum of motor dysfunction of the study population and is less affected by floor or ceiling effects.

The nonclinical impairment measures recorded by robotic devices are positional, for example, tracking error and both isometric force, when locked, and force during movement. Additionally data is produced that demonstrates the relationship between FES and time of the intervention.

Electromyographic (EMG) is also used as an outcome measure in the planar study, and is defined as the study of muscle function through the inquiry of the electrical signal the muscles emanate [S13]. Surface EMG provides a simple noninvasive way to assess general muscle activation during performance of a task, is considered suitable for use with neurological patients [S14], and can aid in determining the intensity and timing of muscular activation and contraction, but is not able to distinguish between concentric or eccentric muscle activity.

Once raw EMG data is collected, data processing typically includes filtering, rectification, and smoothing. A process of normalization is used to compare between different individuals, muscles, or between the same muscles on different occasions. The level of unassisted error tracking of a set of four trajectories was conducted at the beginning and end of each treatment session. Prior to and after the intervention FMA, ARAT, and the ability to apply isometric force in six directions, respectively, are assessed. In order to identify underlying changes in muscle activation patterns, sessions are conducted before and after the intervention when the patients undertake nine tracking tasks with surface EMG recorded from seven muscles in their impaired shoulder and arm, and compared with activation patterns identified from neurologically intact participants in preliminary work. After both the planar and three-dimensional (3-D) interventions, participant perceptions of each iterative learning control system and intervention are sought.

REFERENCES
[S9] R. C. Lyle, "A performance test for assessment of upper limb function in physical rehabilitation treatment and research," Int. J. Rehab. Res., vol. 4, no. 4, pp. 483–492, 1981.
[S10] A. R. Fugl-Meyer, L. Jaasko, I. Leyman, S. Olsson, and S. Steglind, "The post-stroke hemiplegic patient. 1. A method for evaluation of physical performance," Scand. J. Rehab. Med., vol. 7, no. 1, pp. 13–31, 1975.
[S11] J. Sanford, J. Moreland, and L. R. Swanson, "Reliability of the Fugl-Meyer assessment for testing motor performance in patients following stroke," Phys. Ther., vol. 73, no. 7, pp. 447–454, 1993.
[S12] R. Teasell, N. Foley, K. Salter, R. S. Bhogal, N. Bayona, J. Jutai, and M. Speechley. (2007). Evidence based review of stroke rehabilitation. [Online]. Available: http://www.ebrsr.com
[S13] J. V. Basmajian and C. J. de Luca, Muscles Alive, 5th ed. Baltimore, MD: Williams and Wilkins, 1985.
[S14] S. Hesse, "Locomotor therapy in neurorehabilitation," Neurorehabilitation, vol. 16, no. 3, pp. 133–139, 2001.

from 38 to 77 years with a mean age of 52 years. Participants had suffered strokes ranging eight months to 8.4 years, mean four years, prior to recruitment to the study; three were affected on the right-side and two on the left-side. Patients one year beyond the stoke occurring are not likely to recover all lost functionality but improvement to a lower level could also have benefits and, for example, enable them to live independently.

The intervention forming the clinical trials consisted of either 18 or 25 treatment sessions where participants practiced planar reaching tasks augmented by responsive FES of the triceps brachii muscle. Results from applying the stimulation to a stroke patient to assist tracking of the required trajectory are given in Figure 12(a) and (b), which show typical changes in the angle of the shoulder and elbow, respectively, over the duration of the supplied trajectory. Figure 12(c) shows the FES pulse-width that is applied using ILC to produce the assisted movements.

For each participant, the change in tracking error data over the four different unassisted tracking trajectories performed at the beginning of each treatment session is shown in Figure 13, these vary in orientation, duration and length
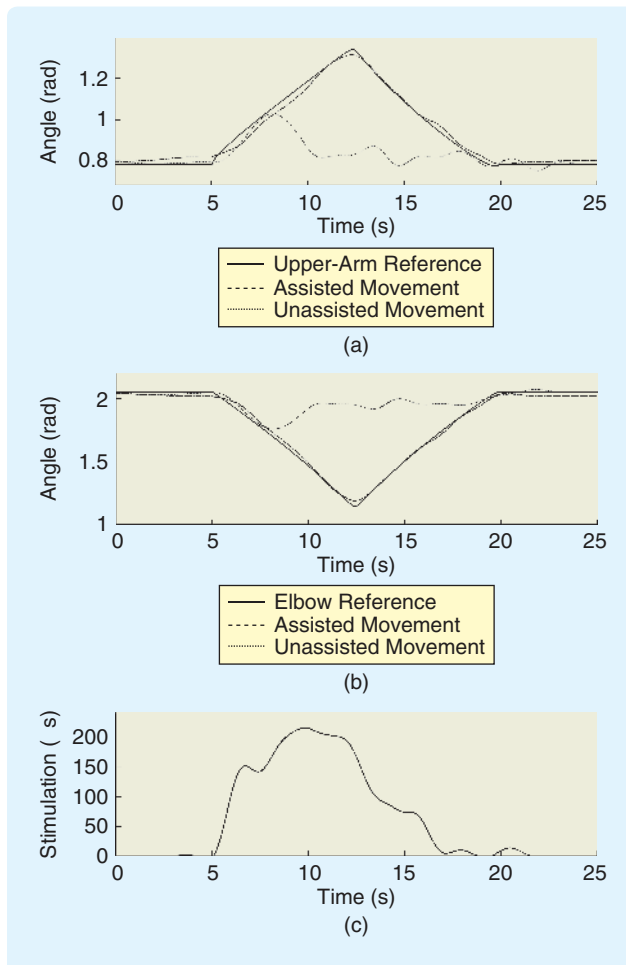
FIGURE 12 Results from applying the stimulation to a stroke patient to assist tracking of a required trajectory, where (a) and (b) show the changes in the angle of the shoulder and elbow, respectively, over the duration of the supplied trajectory. In the plots, the solid line shows the ideal movements that would be required to complete the trajectory, the dotted line represents unassisted movement, and the dashed line shows movement assisted by functional electrical stimulation (FES). Part (c) shows the FES pulse-width that is applied using iterative learning control to produce the assisted movements. During the 5-s countdown period, before the target movement starts, there is minimal stimulation. On the reach component of the trajectory, from 5 to 12.5-s, stimulation increases rapidly and there is a delay period of approximately 2-s between the stimulation peak and the peak shoulder and elbow angle, associated with the biomechanical response to stimulation.

[35]. During these tasks the patient received neither FES nor assistance from the robot. Although the trend for participants is a decrease in tracking error over time, the change is not monotonic, that is, adjacent values may increase. The tracking error decreased most for participants three and five across all trajectories over the intervention. The improvement in unassisted tracking is statistically significant in three of the four tasks [35].

The clinical results of the study are given in [35] which reports significant changes in the outcome measures, error tracking, isometric muscle force, percentage maximum level of stimulation required to correct error, and muscle activation patterns, respectively, for the five chronic stroke participants taking part in the intervention. The ILC system takes into account that the effect of FES is enhanced when associated with the participant's intention to move [6] and that to maximize plasticity stroke participants need to work at their maximum effort in planning and executing tasks during rehabilitation interventions. Although systems have been developed where electrical stimulation is triggered by muscle activity [64], they do not allow feedback to adjust stimulation parameters during tasks, which is a drawback compared with the ability of the training modalities available during robotic assistance to promote voluntary activity [65]. By modifying the gain applied to the ILC update in accordance with the observed error, the ILC system adjusted the level of assistance in response to the users' performance, and so provided only the minimum level of stimulation needed to assist the participant in performing the task to a specified level of accuracy. During the intervention, the error tracking remained within a limited range, specifically less than 15 mm, and the FES required to achieve this error tracking reduced over the course of the intervention. Thus, the balance of FES and voluntary effort required to perform the reaching task changed, with the participants proportionally contributing greater voluntary movement, indicating that motor learning had occurred [35].

The effectiveness of any rehabilitation critically depends on participant perspectives of the procedures and equipment used [66]. Currently there is no generic evaluation tool available to be used across different rehabilitation robot systems. Consequently, participant comments were recorded during the intervention sessions and subsequently a question set developed to explore effectiveness, acceptability, and usability of the ILC system. The question set was administered by a health psychologist to the five stroke participants, and found to be easy to interpret. The findings from this study using a robotic workstation and FES are congruent with other studies [67]–[69], robot-assisted therapy is well accepted and tolerated by the patients. Patients' comments on the best aspects of the study could be separated into physical and psychological benefits, research interaction, being involved, feedback, and enjoyment.

The results of this feasibility study demonstrate that the ILC-based intervention is capable of delivering significant improvements in unassisted error tracking, isometric force, and reduction of impairments as measured using accepted clinical assessment procedures. Additionally, the stroke participants accepted and tolerated the intervention well. The results add to the growing body of evidence that suggests that robotic or FES interventions can be used both to provide objective assessments, before, during, and after an intervention, in addition to being an accepted and well-tolerated treatment that results in changes in impairment levels. In engineering terms, the next stage is to determine
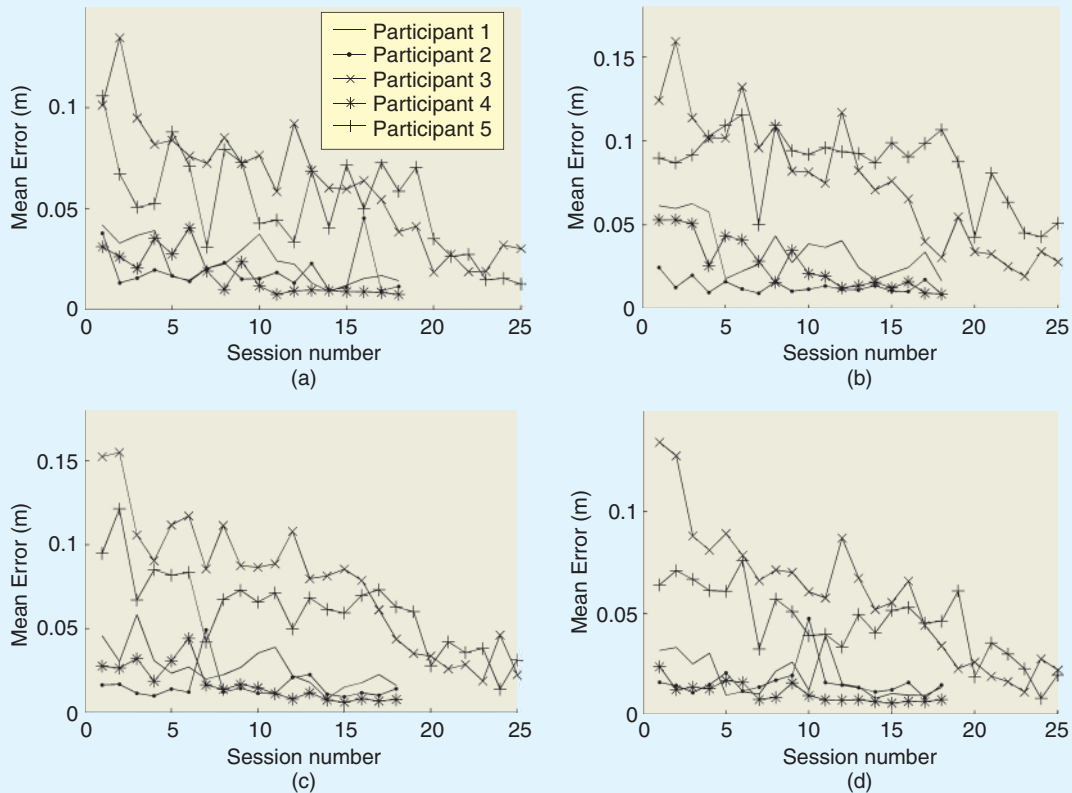
FIGURE 13 Clinical intervention results for planar iterative learning control system: Tracking error data with no functional electrical stimulation assistance as a measure of patient improvement following treatment. For each participant, the change in tracking error data over the four different unassisted tracking trajectories performed at the beginning of each treatment session is shown. Although the trend for participants is a decrease in tracking error over time, the change is not monotonic and adjacent values may increase. The tracking error decreased most for participants three and five across all trajectories over the intervention.

if this approach can be extended to more complex 3-D movements, as discussed in the next section.

ITERATIVE LEARNING CONTROL OF THE UNCONSTRAINED UPPER LIMB

In the work described above, the patient's forearm is constrained to lie in a horizontal plane. The resulting simplification to the underlying biomechanical model enables the development of a simple linearizing controller, and the subsequent implementation of linear ILC algorithms which generally have well defined convergence properties. To maximize the treatment's potential for rehabilitation, it is necessary to use a wider range of more functional movements, which more closely resemble the tasks necessary for daily living [35] and are aligned with the activity-based ARAT measures. This section develops the previous model of the arm to remove the planar forearm constraint, permitting unconstrained movement, and applies ILC to the resulting system.

Stimulated Arm Model

When providing assistive FES during unconstrained 3-D upper-limb reaching movements, FES must be applied using a controlled environment to reduce fatigue and ensure safety and comfort across a broad spectrum of patient abilities. There exist many exoskeletal robotic systems capable of providing such support although very few have been combined with FES, and fewer still with model-based FES control schemes. Here a commercially available device is selected, but the ILC algorithms may be applied to a range of such supports. The mechanical exoskeleton employed is shown in Figure 14 and has two springs incorporated in the mechanism to provide support to overcome gravity. This passive unweighing device allows patients to focus practice on the impaired muscles rather than those acting against gravity. While it is supplied with its own broad range of virtual reality tasks, these are not suitable for controller evaluation and a custom task display system has instead been developed. The patient is seated with their impaired arm strapped into the mechanical unweighing device, whose segmental lengths and degree of antigravity support are adjusted for each user. Joint positional data
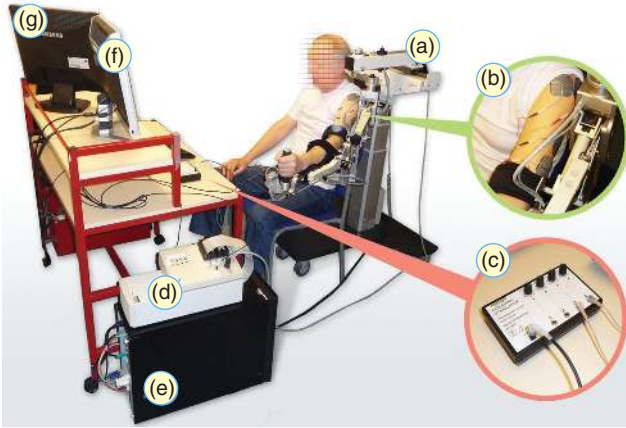
FIGURE 14 Three-dimensional iterative learning control system components: (a) unweighing robotic device, (b) surface electrodes on triceps and anterior deltoid, (c) functional electrical stimulation module, (d) real-time processor and interface module, (e) PC, (f) monitor displaying task, and (g) operator monitor.

the exoskeleton support, where the joint variables $\mathbf{q}_a = [\vartheta_1, \vartheta_2, \vartheta_3, \vartheta_4, \vartheta_5]^T$ correspond to the measured joint angles. Note that the parallelogram structure of the upper-arm section results in $\vartheta_3 = -\vartheta_3'$. The human arm is shown in Figure 15(c), and since it is strapped to the support within the necessary joint ranges there exists a unique bijective transformation between their coordinate sets, given by $\mathbf{q}_u = \mathbf{f}_a(\mathbf{q}_a)$. Here $\mathbf{q}_u = [\vartheta_a, \vartheta_b, \vartheta_c, \vartheta_d, \vartheta_e]^T$ contains the anthropomorphic variables shown in Figure 15(c). Using this relationship, application of Lagrangian analysis produces a dynamic model of the combined robotic and human arm systems given in terms of anthropomorphic coordinates as

$$\mathbf{B}_u(\mathbf{q}_u)\ddot{\mathbf{q}}_u + \mathbf{C}_u(\mathbf{q}_u, \dot{\mathbf{q}}_u)\dot{\mathbf{q}}_u + \mathbf{F}_u(\mathbf{q}_u, \dot{\mathbf{q}}_u) + \mathbf{G}_u(\mathbf{q}_u) + \mathbf{K}_u(\mathbf{q}_u)$$
$$= \tau_u(\mathbf{u}, \mathbf{q}_u, \dot{\mathbf{q}}_u) - \mathbf{J}_u^T(\mathbf{q}_u)\mathbf{h}, \qquad (11)$$

where $\mathbf{B}_p, \mathbf{C}_p \in \mathcal{R}^{5 \times 5}$ are the inertial and Coriolis matrices, respectively, for the 3-D system, $\mathbf{G}_u \in \mathcal{R}^5$ is the vector of moments produced by gravity, and $\mathbf{K}_u \in \mathcal{R}^5$ is the vector of moments produced by the unweighing action where [70] gives a full description of the individual components. The nonconservative forces assume the same form as in the planar case, and hence $\mathbf{F}_u(\mathbf{q}_u, \dot{\mathbf{q}}_u) = [F_a(\vartheta_a, \dot{\vartheta}_a), \ldots F_e(\vartheta_e, \dot{\vartheta}_e)]^T$, whose components incorporate friction and spasticity. The vector due to stimulated muscle $\tau_u(\mathbf{u}, \mathbf{q}_u, \dot{\mathbf{q}}_u) = [0, \tau_b(\mathbf{u}_b, \vartheta_b, \dot{\vartheta}_b), 0, 0, \tau_e(\mathbf{u}_e, \vartheta_e, \dot{\vartheta}_e)]^T$ contains elements of the form (5) in which $\mathbf{u}_b(t)$ and $\mathbf{u}_e(t)$ are the electrical stimulation sequences applied to the triceps and anterior deltoid muscles, respectively, and

provided by resolvers mounted on the support mechanism are transferred to the interface module, which connects external devices to the real-time hardware.

To increase potential for rehabilitation, FES is applied to both the anterior deltoid and triceps muscles in accordance with the clinical objective of providing more assistance, a greater degree of feedback, enabling more accurate movements and ensuring more muscles are usefully activated.

The biomechanical system comprises the human arm and exoskeleton mechanical support system shown in Figure 15(a). Figure 15(b) shows the kinematic structure of
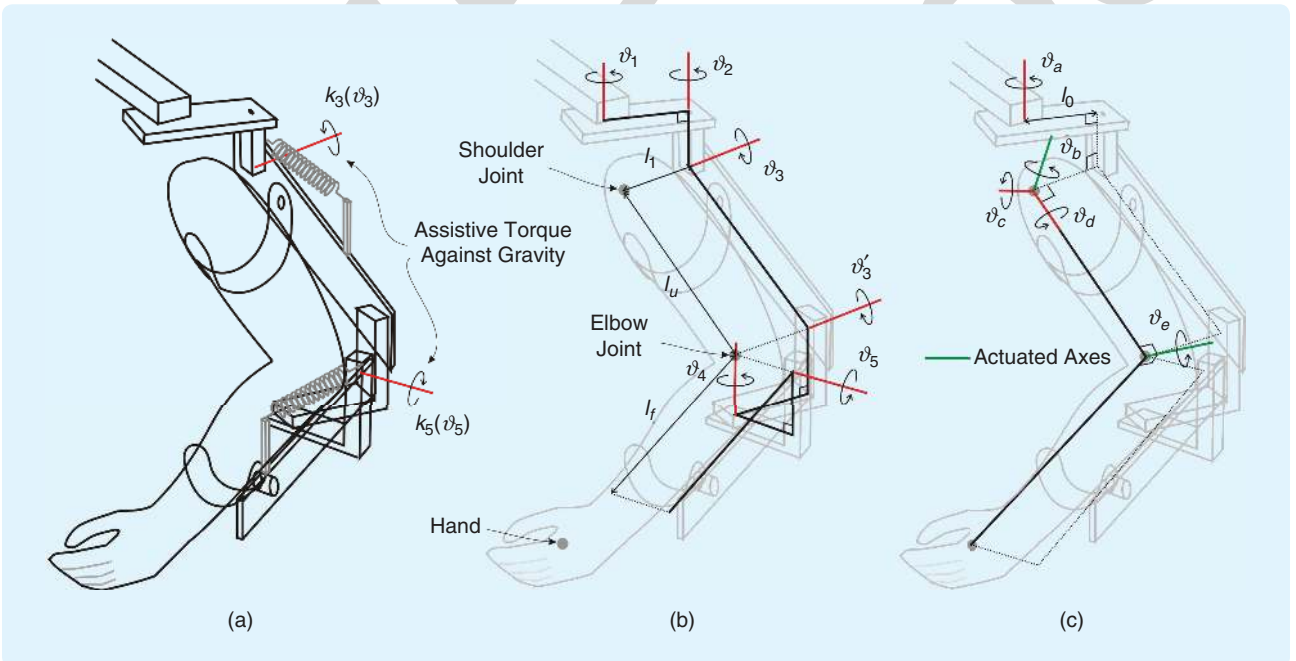

FIGURE 15 Kinematic system relationships: (a) combined system, (b) unweighing robotic device, and (c) human arm.

$u = [u_a, u_b, u_c, u_d, u_e]^T$. The term h represents a vector of external forces and torques applied by the therapist using a handle mounted on a sensor attached to the robotic support. This is only used during identification tests. The model (11) is used by the FES control system to calculate a control signal that results in accurate tracking of a reference trajectory. Since assistive torque is applied about the ϑ_b and ϑ_e axes only, the system is underactuated. When applied during the treatment of patients, the controller assists tracking about ϑ_b and ϑ_e alone, and, in response to clinical guidelines, it is assumed that the patient has sufficient control over the remaining axes to adequately perform the task.

Unlike the planar case, here it is not feasible to display a real world tracking task in 3-D and therefore a virtual task is displayed to the patient to ensure clarity, with provision for additional visual instructions and performance feedback. The patient's screen runs a 3-D virtual reality environment which displays a graphic of their arm in real time, together with the trajectory tracking task, and is shown in Figure 16. The aim of the tracking task is for the patient to follow a sphere which travels along the trajectory at various speeds, while FES controllers designed using the biomechanical system (11) assist their completion. The graphic of the patient's hand changes color to indicate their current error level. Feedback of performance is also given by an error percentage score displayed after each set of trials. A graphic of the initial arm position is displayed to ensure accurate resetting of the system at the start of each trial.

Nine custom reference trajectories are generated for each participant, producing tracking tasks which extend the arm out in front of the patient in response to clinical need. These are calculated using their identified workspace to establish the maximal arm extension directly in front of them, and out to their affected side. By interpolating these two points, a third intermediate point is then generated. Each reference starts from an initial point close to the patient's body, and extends 60, 80, and 100% of the distance to one of these points. The task comprises reaching out to one of the end-point locations, with the fixed trajectories for each of the five joints generated by scaling a third-order ramp signal of 10-s duration and adding an offset, so that it smoothly connects the required start and end joint angles. This results in the vector of reference trajectories $q_u^*(t) = [\vartheta_a^*(t), \vartheta_b^*(t), \vartheta_c^*(t), \vartheta_d^*(t), \vartheta_e^*(t)]^T$ where the presence of nonfixed $\vartheta_a^*(t)$, $\vartheta_c^*(t)$, and $\vartheta_d^*(t)$ components makes the task more natural to the patients, who can use their remaining voluntary effort to move these joints. An example of the reaching tasks used during testing and in clinical trials is given in Figure 17.

3-D Control Schemes
First the phase-lead algorithm (9) is applied to this 3-D case by considering the system to be composed of two single-input, single-output (SISO) systems, the control and move-

FIGURE 16 Three-dimensional virtual reality environment for patients, showing reaching trajectory comprising a sphere moving along a path and a graphic of the arm. Visual feedback provided by changing sphere color.
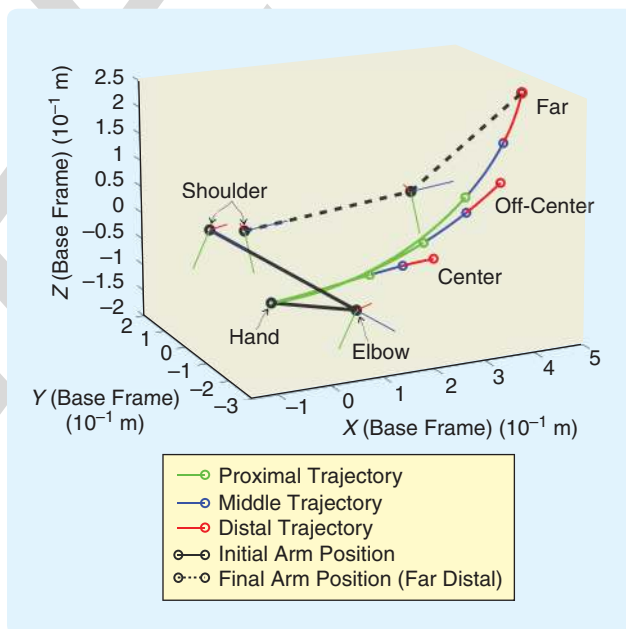

FIGURE 17 Reference trajectories used for the three-dimensional rehabilitation system.

ment of forearm and upper arm are independent of each other. Since FES is applied only about ϑ_b and ϑ_e, L is multiplied by the matrix $\text{diag}\{0, 1, 0, 0, 1\}$, and the error is given by $e_k = q_u^* - q_u$. As illustrated in Figure 18 ILC operates in conjunction with a feedback controller given by $\xi_k/e_k = C(s)$ that provides baseline tracking and disturbance rejection. In operation the phase-lead controller performs best when the system approximates a simple time delay and with an appropriately tuned feedback controller can ensure rapid convergence over initial trials [71]. As in the planar case, the problem of high frequency components gradually increasing when a large number of trials are performed can
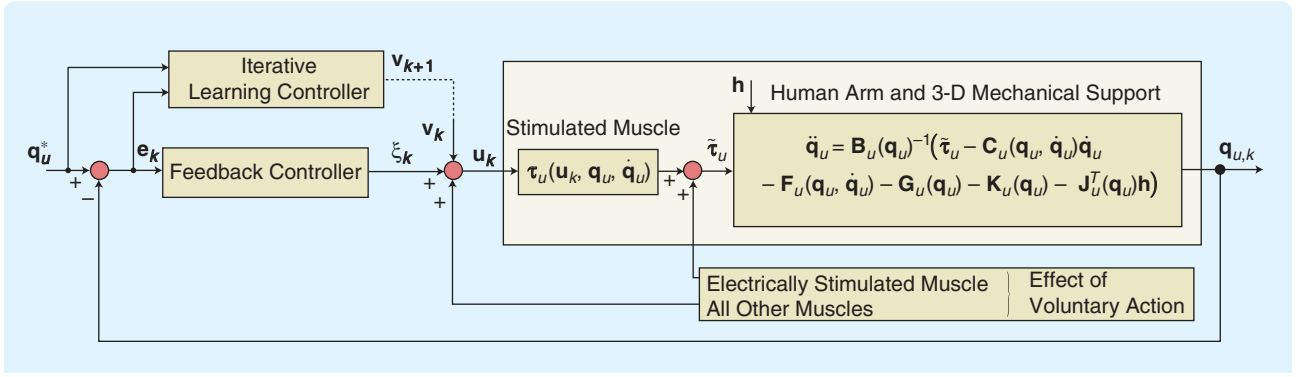
FIGURE 18 Block diagram representation of the iterative learning control (ILC) scheme for the three-dimensional (3-D) rehabilitation system.

always be addressed through use of a zero-phase filter applied to the error or control input, however the low number of trials performed means that it is unnecessary in the present application.

In contrast to the simpler phase-lead approach, Newton method-based ILC [72] uses the full model in the calculation of the new input. Firstly the closed-loop connection of the system (11) and feedback controller is written as the following discrete-time state-space model

$$
\begin{aligned}
\mathbf{x}_k(t+1) &= \mathbf{f}[\mathbf{x}_k(t), \mathbf{v}_k(t)], \\
\mathbf{q}_{u,k}(t) &= \mathbf{h}[\mathbf{x}_k(t)],
\end{aligned} \tag{12}
$$

where $t \in [0, 1, 2, \ldots, N-1]$ is the sample number, $\mathbf{x}_k(t)$ is the state vector, and $N = T/T_s + 1$ with T_s the sampling frequency. Introducing the vectors

$$
\begin{aligned}
\mathbf{v}_k &= [\mathbf{v}_k(0)^T, \mathbf{v}_k(1)^T, \ldots, \mathbf{v}_k(N-1)^T]^T, \\
\mathbf{q}_{u,k} &= [\mathbf{q}_{u,k}(0)^T, \mathbf{q}_{u,k}(1)^T, \ldots, \mathbf{q}_{u,k}(N-1)^T]^T,
\end{aligned} \tag{13}
$$

and the reference vector

$$
\mathbf{q}_u^* = [\mathbf{q}_u^*(0)^T, \mathbf{q}_u^*(1)^T, \ldots, \mathbf{q}_u^*(N-1)^T]^T, \tag{14}
$$

the Newton method-based ILC update takes the form

$$
\mathbf{v}_{k+1} = \mathbf{v}_k + \mathbf{g}'(\mathbf{v}_k)^{-1}\mathbf{e}_k, \tag{15}
$$

where $\mathbf{e}_k = \mathbf{q}_u^* - \mathbf{q}_{u,k}$ is the tracking error. The term $\mathbf{g}'(\mathbf{v}_k)$ is equivalent to the system linearization around $\mathbf{v}_k$, with the system $\tilde{\mathbf{q}}_u = \mathbf{g}'(\mathbf{v}_k)\tilde{\mathbf{v}}$ corresponding to the linear time-varying (LTV) system

$$
\begin{aligned}
\tilde{\mathbf{x}}(t+1) &= \mathbf{A}(t)\tilde{\mathbf{x}}(t) + \mathbf{B}(t)\tilde{\mathbf{v}}(t), \\
\tilde{\mathbf{q}}_u(t) &= \mathbf{C}(t)\tilde{\mathbf{x}}(t) + \mathbf{D}(t)\tilde{\mathbf{v}}(t), \quad t = 0, 1, \ldots, N-1
\end{aligned} \tag{16}
$$

with

$$
\mathbf{A}(t) = \left(\frac{\partial \mathbf{f}}{\partial \mathbf{x}}\right)_{\mathbf{v}_k(t), \mathbf{x}_k(t)}, \qquad \mathbf{B}(t) = \left(\frac{\partial \mathbf{f}}{\partial \mathbf{v}_k}\right)_{\mathbf{v}_k(t), \mathbf{x}_k(t)},
$$

$$
\mathbf{C}(t) = \left(\frac{\partial \mathbf{h}}{\partial \mathbf{x}}\right)_{\mathbf{v}_k(t), \mathbf{x}_k(t)}, \qquad \mathbf{D}(t) = \left(\frac{\partial \mathbf{h}}{\partial \mathbf{v}_k}\right)_{\mathbf{v}_k(t), \mathbf{x}_k(t)}. \tag{17}
$$

The term $\mathbf{g}'(\mathbf{v}_k)^{-1}$ in (15) is computationally expensive and may be singular or contain excessive amplitudes and high frequencies. To overcome this difficulty, introduce
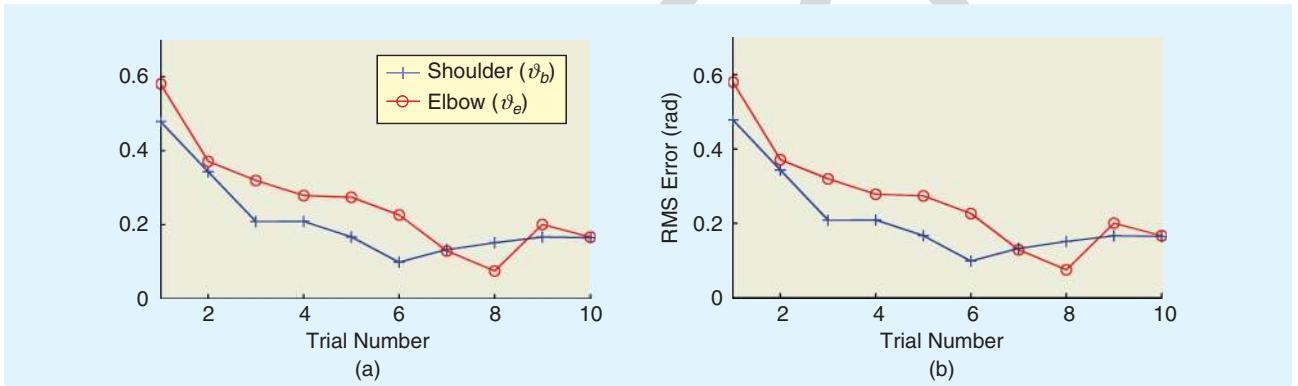

FIGURE 19 Root mean square (RMS) error plots for (a) participant one and (b) participant two using phase-lead iterative learning control.

$$\mathbf{e}_k = \mathbf{g}'(\mathbf{v}_k)\Delta\mathbf{v}_{k+1}, \qquad (18)$$

and then $\Delta\mathbf{v}_{k+1} = \mathbf{v}_{k+1} - \mathbf{v}_k$ equals the input that forces the LTV system (16) to track the error $\mathbf{e}_k$. This is itself an ILC problem and can be solved in between experimental trials using any ILC algorithm that converges globally. In this article norm optimal ILC [73] is considered, with the input and output on trial j denoted by $\mathbf{e}_{k,j}$ and $\Delta\mathbf{v}_{k+1,j}$, respectively. On trial $j + 1$, the trade off between minimizing the tracking error, $\mathbf{e}_k - \mathbf{e}_{k,j}$ and the change in control input $\Delta\mathbf{v}_{k+1,j+1} - \Delta\mathbf{v}_{k+1,j}$, is represented by the cost function

$$
\begin{aligned}
\mathbf{J}_{j+1} = &\sum_{t=0}^{N-1} (\mathbf{e}_k - \mathbf{e}_{k,j})(\mathbf{t})^{\mathsf{T}}\mathbf{Q}(\mathbf{e}_k - \mathbf{e}_{k,j})(\mathbf{t}) \\
&+ \sum_{t=0}^{N-1} (\Delta\mathbf{v}_{k+1,j+1} - \Delta\mathbf{v}_{k+1,j})(\mathbf{t})^{\mathsf{T}}\mathbf{R}(\Delta\mathbf{v}_{k+1,j+1} - \Delta\mathbf{v}_{k+1,j})(\mathbf{t}),
\end{aligned}
$$
$$(19)$$

where $\mathbf{Q}$ and $\mathbf{R}$ are symmetric positive definite weighting matrices of compatible dimension. The ILC computation is stopped after 100 trials or after the error reaches a preset threshold. The input obtained, $\Delta\mathbf{v}_{k+1,j}$, is then used to approximate $\Delta\mathbf{v}_{k+1}$ in (15) to generate the control input for the next trial.

Experimental Results with Unimpaired Subjects

The phase-lead ILC and Newton method-based ILC algorithms have been experimentally implemented on six unimpaired participants as an essential step in obtaining ethical approval for patient trials, and representative results and summary statistics are given in this section. Each participant is seated in the robot, which is adjusted to their individual arm dimensions. Electrodes are positioned over their triceps and anterior deltoid muscles in such a way that maximum movement is generated through application of FES. The stimulation amplitude and maximum pulsewidth are adjusted so that they are within comfortable limits. As discussed in the previous section, the model of the human arm includes two person-dependent parameters that define the position of the anterior deltoid axis,
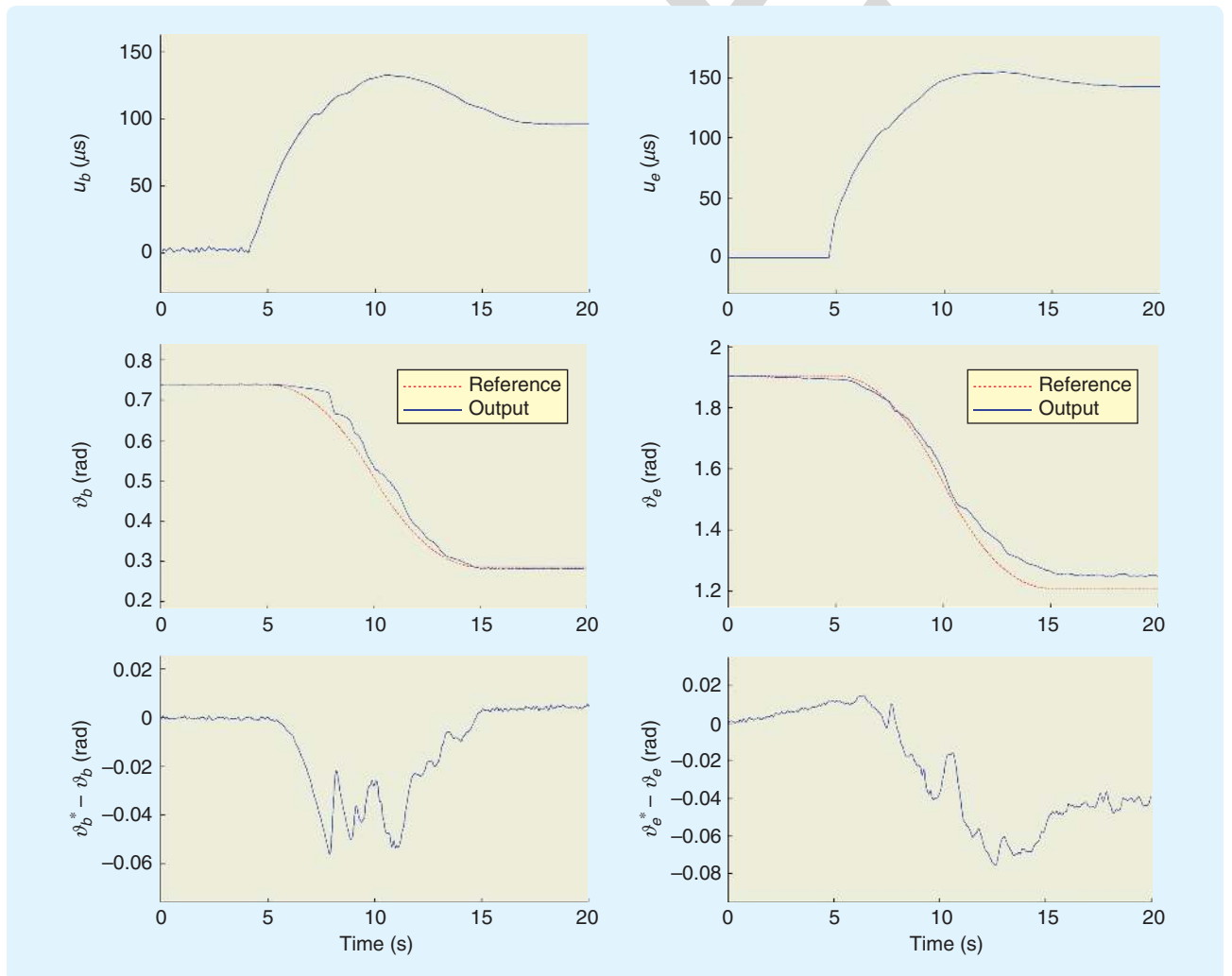

FIGURE 20 Tracking performance for participant one on trial six. Five second padding is applied at the beginning and end of each reaching movement.

TABLE 2 Mean (standard deviation) root mean square (RMS) error for six unimpaired participants undertaking two trajectory tracking exercises using the three-dimensional robot system with no voluntary assistance.

		Trajectory 1		Trajectory 2	
Shoulder RMS error (rad)	Best trial only	0.2415	(0.0693)	0.0574	(0.0557)
	Mean of first six trials	0.0949	(0.0906)	0.1691	(0.1609)
Elbow RMS error (rad)	Best trial only	0.0721	(0.0700)	0.0837	(0.0900)
	Mean of first six trials	0.1480	(0.1327)	0.2189	(0.1723)

which is fixed with respect to the shoulder as shown in Figure 15(c). These are determined before experiments are carried out, by simply applying FES to the anterior deltoid and recording the resulting movements of the human arm. Since the rotation of the human upper arm should then be about the anterior deltoid axis [see Figure 15(c)] this axis is identified by fitting a plane to the elbow position by least mean squares optimization. The vector perpendicular to the plane, which is also through the pivot, then equates to the required anterior deltoid axis [70].

The initial results using the phase-lead ILC algorithm show good performance. Figure 19 gives tracking performance results for two participants. The RMS error is given for both ϑ_b and ϑ_e over 10 trials, where for trial k

$$\text{RMS}_{i,k} = \sqrt{\frac{1}{N}\sum_{t=0}^{N-1}\left(\vartheta_i^*(t) - \vartheta_{i,k}(t)\right)^2}, \quad i = b, e, \tag{20}$$

where N is the number of samples in the discrete representations of the reference $\vartheta_i^*(t)$ and recorded joint angle

sequence $\vartheta_i(t)$. Due to the kinematic redundancy of the task, this is a more reliable measure than the Cartesian end-point error, which was used in the planar case.

The tracking error in the unimpaired study reduces quickly and maintains a low level over latter trials. In some cases the RMS error increases slightly in later trials because the participant's triceps started to suffer from fatigue but the ILC was quickly able to modify the stimulation to maintain a low error. Figure 20 shows tracking performance for the same two participants, illustrating close reference tracking for both controlled angles.

Table 2 provides summary statistics for six unimpaired participants who have undertaken testing. Each participant undertook ILC trials using two trajectories, the first moved their arm out in front of them and the second moved it out and to their side. The average RMS error was calculated for each trajectory and the mean and standard deviation calculated across participants. These calculations were then repeated using the lowest RMS error recorded for each trajectory.

Experimental results using Newton method-based ILC scheme using full knowledge of the system dynamics (11) are also available. Figure 21 shows error norm results over 10 trials of the Newton method-based ILC algorithm for two patients, using a long off center and a medium off center trajectory. The results are representative of all the
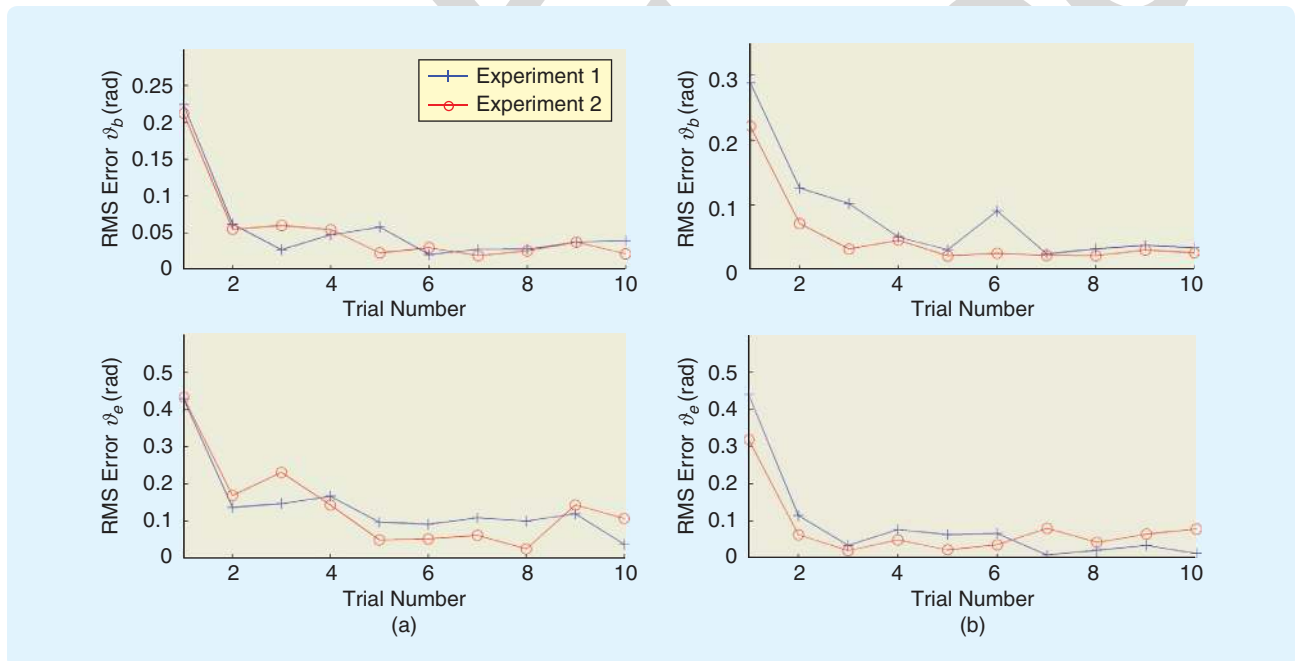

FIGURE 21 Root mean square (RMS) error plots for two participants using Newton method-based iterative learning control: (a) subject one and (b) subject two.
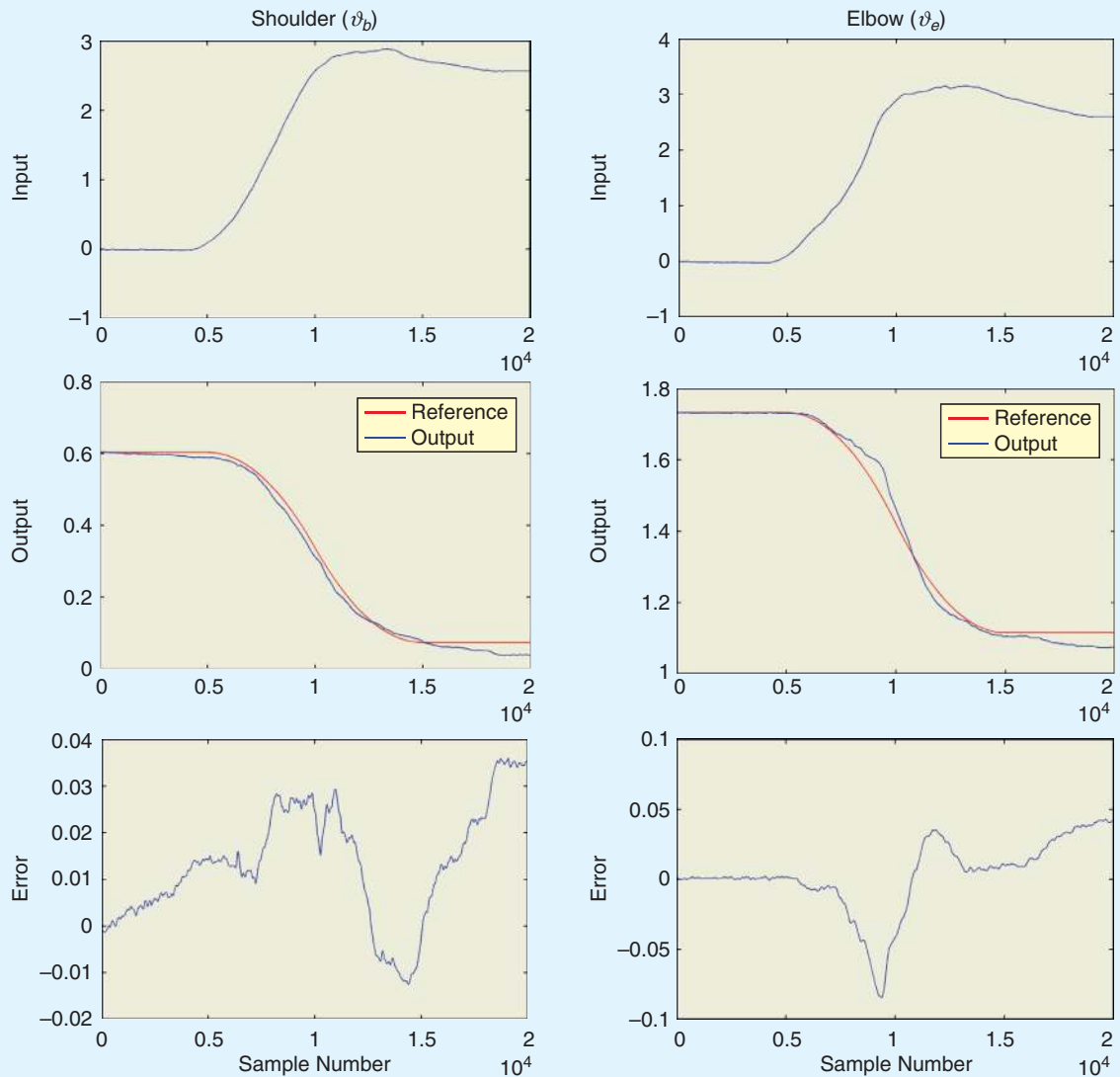
FIGURE 22 Tracking performance of the Newton method-based iterative learning control algorithm.

tasks tested and confirm that accurate tracking is achieved within very few trials. The weighting matrices used in the tests are $Q = 30I$ and $R = I$, respectively. Figure 22 shows representative input, output, and error signals recorded on trial 8 for one participant and confirm that a high level of tracking performance is achieved with an input signal that is not excessive. The theoretical quality of rapid monotonic convergence to zero tracking error is degraded due to inaccuracies in the human arm model which deteriorate performance, motivating development of more accurate identification procedures, and future use of online and recursive techniques. Such identifications routines, however, must be suitable for application within the restrictive conditions of clinical trials, where there is limited set-up time, little opportunity to repeat measurements, and where techniques must yield satisfactory results for a wide range of patients and changing physiological conditions.

CLINICAL ASSESSMENT

Clinical trials using the 3-D system have recently been undertaken. Their form closely replicates those of the planar case, again including five patients with treatment taking place over 18 sessions of 1-h duration. A range of the tasks shown in Figure 17 were selected by the therapist for training using the phase-lead update algorithm to supply assistance. The protocol matched that of the preliminary trials. Assessment again involved pre and post-intervention Fugl-Meyer and ARAT measures, and unassisted tracking with no FES supplied was recorded at the beginning and end of each treatment session using four standardized tasks. Unassisted tracking results are given in Figure 23 and show how the performance increases as the treatment progresses [74] with trends observed that are statistically significant. The Fugl-Meyer scores also showed significant improvement in patients's ability to move; how-
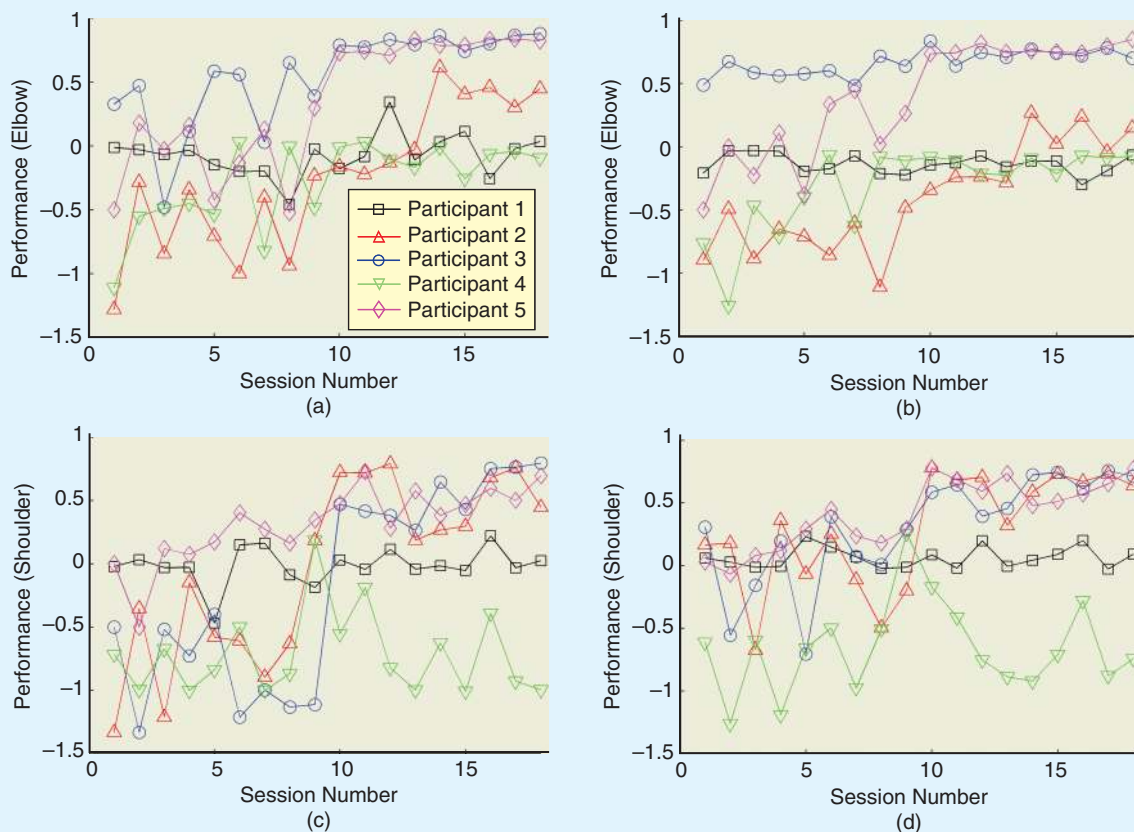
FIGURE 23 Clinical intervention results for three-dimensional iterative learning control system. Unassisted tracking performance for the elbow and shoulder as a function of session for each participant and unassisted task. Part (a) shows elbow tracking performance for the center-distal task; (b) shows elbow tracking performance for the off-center-middle task; (c) shows shoulder tracking performance for the center-distal task; (d) shows shoulder tracking performance for the off-center-middle task. 1 = perfect tracking performance.

ever, this did not transfer to a significant increase in ARAT scores. This is consistent with the planar case and with a number of systematic reviews reporting that robotic therapy reduces motor impairment but does not currently improve functional impairment.

FIGURE 24 From left: Eric Rogers, Ann-Marie Hughes, Jane Burridge, Katie Meadmore, and Chris Freeman.

CONCLUSIONS AND FURTHER RESEARCH

In response to next generation health care needs there is currently significant interest in both rehabilitation robotics and therapeutic application of FES, with a clinically supported need to combine technologies whilst developing controllers for the latter that enable precise control of movement during functional tasks. This article describes how robotic and FES controllers may be integrated to supply complementary assistance driven by clinical need. A scheme that yielded significant clinical results is first described, and then the methodology generalized to allow dual robotic and FES controller derivation during more functional tasks involving unconstrained arm movement.

The progress reported in this article forms a critical first step in the development of FES controllers for full reach and grasp movements involving shoulder, elbow, wrist, and hand stimulation during fully functional movements and there are many areas for further research in both engineering and clinical assessment before uptake by practicing medical professionals is possible. In the latter aspect, the use of any new medical intervention or treatment will require randomized control trials. The low number of
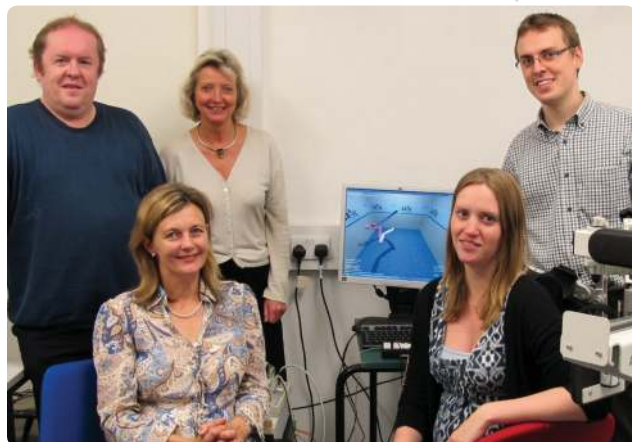
patients used in the clinical trials in this article show feasibility and a sample size calculation can be conducted to establish exactly how many patients would be needed to conduct a randomized controlled trial.

In engineering terms, further development of the algorithms used is required. One area for short to medium term research is the question of how to select the reference signal for each patient. At present this is done by a physiotherapist from an assessment of the patient without any decision support tools and if the task given to patients is already within their capability then no rehabilitation takes place as a result of the treatment. Conversely, a task which is far beyond current capabilities can lead to serious patient demotivation. An open question then is whether the region of effective operation can be estimated from pre-assessment and measurement data.

The ability to use the hand is an integral component of the ARAT and other functional outcome measures, and therefore clearly motivates development of ILC for functional control of the hand and wrist. As the movement complexity increases, there is more emphasis on model-based approaches to provide optimal performance which maximizes effectiveness of therapy. However there are virtually no model-based control approaches for the hand and wrist which have been applied clinically [16], making this an important area for further research. Additionally, as discussed previously, the accurate extraction and incorporation of voluntary effort into the model using EMG signals is still an open problem.

Effective FES-based rehabilitation demands that patients are assisted during functional tasks in a manner that mimics their performance in the absence of impairment. There exists extensive literature on motor control for both unimpaired and stroke subjects which provide kinematic analysis of movement, for example framing tasks as constrained optimization problems [75]. As perhaps the only model-based upper-limb FES control approach that has been employed clinically, the ILC framework holds potential as a route to embed existing motor control research within rehabilitation. However, such exploitation requires development of ILC laws which do not comprise the tracking of fixed reference trajectories defined over the task duration, but rather incorporate point-to-point movements with embedded input and output constraints [76]. These constraints may also reflect explicit coordination acting between joint variables and the presence of muscle synergies.

Furthermore, it is also necessary to adapt the task objective in response to identified system knowledge and ongoing performance, incorporating expert knowledge, clinical data, prior performance relationships, and established task progression models. Lastly the robust stability of the overall system, incorporating adaptive model identification, ILC learning, and task adaption loops must be established in a general framework.

AUTHOR INFORMATION

Chris T. Freeman (cf@ecs.soton.ac.uk) is lecturer in applied control, School of Electronics and Computer Science, University of Southampton, U.K. He received the B.Sc. degree in mathematical sciences from the Open University, the B.Eng. degree in electromechanical engineering from the University of Southampton, and the Ph.D. degree in control systems from the same institution. His research interests are in biomechanics, motor learning and control, iterative learning, and repetitive control theory and their experimental application to industrial systems and stroke rehabilitation. He can be contacted at the School of Electronics and Computer Science, University of Southampton, Southampton, SO17 1BJ, U.K.

Eric Rogers is professor of control systems theory and design, School of Electronics and Computer Science, University of Southampton, U.K. He received the B.Sc. degree in mechanical engineering from Queen's University Belfast, U.K.; the masters and Ph.D. degrees in control systems from the University of Sheffield, U.K.; and the D.Sc. degree in control systems from Queen's University Belfast, U.K. His research interests are in multidimensional systems theory, systems with repetitive dynamics, iterative learning control theory and experimental verification, and flow control.

Ann-Marie Hughes is a senior research fellow in the faculty of health sciences, University of Southampton, U.K. She received the B.Sc. degree in chemistry from the University of Exeter, U.K., and the Ph.D. degree in control systems for stroke rehabilitation from the University of Southampton, U.K. Her research interests are in the application of new technologies to enhance recovery following neurological injury or disease.

Jane H. Burridge is professor of restorative neuroscience, Faculty of Health Sciences, University of Southampton, U.K. She trained as a physiotherapist and then received the Ph.D. degree from the University of Southampton, U.K. Her research interests concern understanding how motor control is affected by lesions of the central nervous system and the development and application of innovative technologies for the recovery of functional movement following stroke.

Katie L. Meadmore is a research fellow in the School of Electronics and Computer Science, University of Southampton, U.K. She received her B.Sc. degree in psychology and Ph.D. on visual spatial processing and ageing from the School of Psychology, University of Southampton. Her research interests are in using eye movement methodology and health technology to understand visual cognition and rehabilitation in ageing populations and neurological disorders.

REFERENCES
[1] J. J. M. F. van der Putten, J. C. Hobart, J. A. Freeman, and A. J. Thompson, "Measuring change in disability after inpatient rehabilitation: Comparison

of the responsiveness of the Barthel index and the functional independence measure," J Neurol. Neurosurg. Psychiatry, vol. 66, pp. 480–484, 1999. <AU: Please provide the issue number.>

[2] H. T. Hendricks, J. van Limbeek, A. C. Geurts, and M. J. Zwarts, "Motor recovery after stroke: A systematic review of the literature," Arch. Phys. Med. Rehab., vol. 83, pp. 1629–1637, 2002. <AU: Please provide the issue number.>

[3] National Audit Office. (2004). Reducing brain damage: Faster access to better stroke care. HC 452 [Online]. Available: http://www.nao.org.uk/publications/0506/reducing_brain_damage.aspx

[4] C. J. Winstein, D. K. Rose, S. M. Tan, R. Lewthwaite, H. C. Chui, and S. P. Azen, "A randomized controlled comparison of upper-extremity rehabilitation strategies in acute stroke: A pilot study of immediate and long-term outcomes," Arch. Phys. Med. Rehab., vol. 85, pp. 620–628, 2004. <AU: Please provide the issue number.>

[5] R. A. McGill, Motor Learning—Concepts and Applications. New York: McGraw-Hill, 1998.

[6] J. R. De Kroon, M. J. Ijzerman, J. J. Chae, G. J. Lankhorst, and G. Zilvold, "Relation between stimulation characteristics and clinical outcome in studies using electrical stimulation to improve motor control of the upper extremity in stroke," J. Rehab. Med., vol. 37, no. 2, pp. 65–74, 2005.

[7] V. M. Pomeroy, L. King, A. Pollack, A. Baily-Hallon, and P. Longhorne. (2006). Electrostimulation for promoting recovery of movement or functional ability after stroke. Cochrane Database Syst. Rev. [Online]. (2). Available: http://onlinelibrary.wiley.com/o/cochrane/clsysrev/articles/CD003241/frame.html

[8] G. B. Prange, M. A. Jannick, C. G. M. Groothuis-Oudshoorn, H. Hermens, and M. J. Ijzerman, "Systematic review of the effect of robot-aided therapy on recovery of the hemiparetic arm after stroke," J. Rehab. Res. Dev., vol. 43, pp. 171–184, 2006. <AU: Please provide the issue number.>

[9] G. Kwakkel, B. J. Kollen, and H. I. Krebs, "Effects of robot-assisted therapy on upper limb recovery after stroke: A systematic review," Neurorehab. Neural Repair, vol. 22, no. 2, pp. 111–121, 2008.

[10] Intercollegiate Working Party for Stroke, National Clinical Guidelines for Stroke. London: Royal College of Physicians, 2004.

[11] J. R. de Kroon, J. H. van der Lee, M. J. Izerman, and G. J. Lankhorst, "Therapeutic electrical stimulation to improve motor control and functional abilities of the upper extremity after stroke: A systematic review," Clin. Rehab., vol. 16, pp. 350–360, 2002. <AU: Please provide the issue number.>

[12] J. H. Burridge and M. Ladouceur, "Clinical and therapeutic applications of neuromuscular stimulation: A review of current use and speculation into future developments," Neuromodulation, vol. 4, no. 4, pp. 147–154, 2001.

[13] R. A. Schmidt and T. D. Lee, "Motor learning," in Motor Control and Learning: A Behavioral Emphasis, Part 3. Human Kinetics, 1999, pp. 261–285. <AU: Please provide the editor name(s) and publisher location.>

[14] J. R. de Kroon, M. J. Ijzerman, G. J. Lankhorst, and G. Zilvold, "Relation between stimulation characteristics and clinical outcome in studies using electrical stimulation to improve motor control of upper extremity in stroke," J. Rehab. Med., vol. 35, pp. 65–74, 2005. <AU: Please provide the issue number.>

[15] D. N. Rushton, "Functional electrical stimulation and rehabilitation—An hypothesis," Med. Eng. Phys., vol. 1, pp. 75–78, 2003. <AU: Please provide the issue number.>

[16] D. Zhang, T. H. Guan, F. Widjaja, and W. T. Ang, "Functional electrical stimulation in rehabilitation engineering: A survey," in Proc. Convention Rehabilitation Engineering and Assistive Technology, Singapore, 2007, pp. 221–226.

[17] K. J. Hunt, M. Munih, and N. de Donaldson, "Feedback control of unsupported standing in paraplegia—Part I: Optimal control approach," IEEE Trans. Rehab. Eng., vol. 5, no. 4, pp. 331–340, 1997.

[18] K. J. Hunt, R. P. Jaime, and H. Gollee, "Robust control of electrically-stimulated muscle using polynomial H_∞ design," Control Eng. Pract., vol. 9, pp. 313–328, 2001. <AU: Please provide the issue number.>

[19] R. Davoodi and B. J. Andrews, "Computer simulation of FES standing up in paraplegia: A self-adaptive fuzzy controller with reinforcement learning," IEEE Trans. Rehab. Eng., vol. 6, no. 2, pp. 151–161, 1998.

[20] S. Jezernik, R. G. V. Wassink, and T. Keller, "Sliding mode closed-loop control of FES: Controlling the shank movement," IEEE Trans. Biomed. Eng., vol. 51, no. 2, pp. 263–272, 2004.

[21] F. Previdi, T. Schauer, S. M. Savaresi, and K. J. Hunt, "Data-driven control design for neuroprostheses: A virtual reference feedback tuning (VRFT) approach," IEEE Trans. Control Syst. Technol., vol. 12, no. 1, pp. 176–182, 2004.

[22] T. Watanabe, K. Iibuchi, K. Kurosawa, and N. Hoshimiya, "A method of multichannel PID control of two-degree-of-freedom wrist joint movements by functional electrical stimulation," Syst. Comput. Jpn., vol. 34, no. 5, pp. 319–328, 2003.

[23] N. Lan, H. Q. Feng, and P. E. Crago, "Neural network generation of muscle stimulation patterns for control of arm movements," IEEE Trans. Rehab. Eng., vol. 2, no. 4, pp. 213–224, 1994.

[24] P. Tresadern, S. Thies, L. O. Kenney, D. Howard, and J. Y. Goulermas, "Artificial neural network prediction using accelerometers to control upper limb FES during reaching and grasping following stroke," in Proc. 28th Annu. Int. Conf. IEEE Engineering in Medicine and Biology Society, 2006, pp. 2916–2919.

[25] G. Graupe and H. Kordylewski, "Neural network control of neuromuscular stimulation in paraplegics for independent ambulation," in Proc. 19th Annu. Int. Conf. IEEE Engineering in Medicine and Biology Society, 1997, pp. 1088–1091.

[26] G. P. Bratz, R. M. Smith, and G. M. Davis, "Designing an FES control algorithm: Important considerations," in Proc. World Congr. Medical Physics and Biomedical Engineering, Seoul, Korea, 2006, pp. 2848–2851.

[27] C. L. Lynch and M. R. Popovic, "Functional electrical stimulation: Closed-loop control of induced muscle contractions," IEEE Control Syst. Mag., vol. 28, no. 4, pp. 40–50, 2008.

[28] J. R. de Kroon, J. H. van der Lee, M. J. Ijzerman, and G. J. Lankhorst, "Therapeutic electrical stimulation to improve motor control and functional abilities of the upper extremity after stroke: A systematic review," Clin. Rehab., vol. 16, pp. 350–360, 2002. <AU: Kindly provide the issue no.>

[29] J. R. de Kroon, M. J. Ijzerman, J. Chae, G. J. Lankhorst, and G. Zilvold, "Relation between stimulation characteristics and clinical outcome in studies using electrical stimulation to improve motor control of the upper extremity in stroke," J. Rehab. Med., vol. 37, pp. 65–74, 2005. <AU: Kindly provide the issue no.>

[30] J. R. de Kroon and M. J. Ijzerman, "Electrical stimulation of the upper extremity in stroke: Cyclic versus EMG-triggered stimulation," Clin. Rehab., vol. 22, pp. 690–697, 2008. <AU: Kindly provide the issue no.>

[31] R. Thorsen, R. Spadone, and M. Ferrarin, "A pilot study of myoelectrically controlled FES of upper extremity," IEEE Trans. Neural Syst. Rehab. Eng., vol. 9, no. 2, pp. 161–168, 2001.

[32] L. L. Baker, D. R. McNeal, L. A. Benton, B. R. Bowman, and R. L. Waters, Neuromuscular Electrical Stimulation: A Practical Guide, 3rd ed. 1993. <AU: Kindly provide the name and location of the publisher.>

[33] C. T. Freeman, A.-M. Hughes, J. H. Burridge, P. H. Chappell, P. L. Lewin, and E. Rogers, "A model of the upper extremity using FES for stroke rehabilitation," J. Biomech., vol. 131, no. 3, pp. 031011-1–031011-12, 2009.

[34] C. T. Freeman, A.-M. Hughes, J. H. Burridge, P. H. Chappell, P. L. Lewin, and E. Rogers, "Iterative learning control of FES applied to upper extremity for rehabilitation," Control Eng. Pract., vol. 17, no. 3, pp. 368–381, 2009.

[35] A.-M. Hughes, C. T. Freeman, J. H. Burridge, P. H. Chappell, P. L. Lewin, and E. Rogers, "Feasibility of iterative learning control mediated by functional electrical stimulation for reaching after stroke," Neurorehab. Neural Repair, vol. 23, no. 6, pp. 559–568, 2009.

[36] T. Seel, T. Schauer, and J. Raisch, "Iterative learning control for variable pass length systems," in Proc. 18th IFAC World Congr., Milan, Italy, 2011, pp. 4880–4885.

[37] H. Nahrstaedt, T. Schauer, S. Hesse, and J. Raisch, "Iterative learning control of a gait neuroprosthesis," Automatisierungstechnik, vol. 56, no. 9, pp. 494–501, 2008.

[38] J. Bae and M. Tomizuka, "A gait rehabilitation strategy inspired by an iterative learning algorithm," in Proc. 18th IFAC World Congr., Milan, Italy, 2011, pp. 2857–2864.

[39] C. T. Freeman, A.-M. Hughes, J. H. Burridge, P. H. Chappell, P. L. Lewin, and E. Rogers, "A robotic workstation for stroke rehabilitation of the upper extremity using FES," Med. Eng. Phys., vol. 31, no. 3, pp. 364–373, 2009.

[40] A.-M. Hughes, C. T. Freeman, J. H. Burridge, P. H. Chappell, P. L. Lewin, and E. Rogers, "Shoulder and elbow muscle activity during fully supported trajectory tracking in people who have had a stroke," J. Electromyogr. Kinesiol., vol. 20, no. 3, pp. 465–476, 2010.

[41] F. Le, I. Markovsky, C. T. Freeman, and E. Rogers, "Identification of electrically stimulated muscle models of stroke patients," Control Eng. Pract., vol. 18, no. 4, pp. 396–407, 2010.

[42] D. Popovic and M. Popovic, "Tuning of a nonanalytical hierarchical control system for reaching with FES," IEEE Trans. Bio-Med. Eng., vol. 45, no. 2, pp. 203–212, 1998.

[43] P. E. Crago, R. J. Nakai, and H. J. Chizeck, "Feedback regulation of hand grasp opening and contact force during stimulation of paralysed muscle," IEEE Trans. Bio-Med. Eng., vol. 38, no. 1, pp. 17–28, 1991.

[44] H. J. Chizeck, N. Lan, L. S. Palmieri, and P. E. Crago, "Feedback control of electrically stimulated muscle using simultaneous pulse width and stimulus period modulation," IEEE Trans. Bio-Med. Eng., vol. 38, no. 12, pp. 1224–1234, 1991.

[45] M. S. Hatwell, B. J. Oderkerk, C. A. Sacher, and G. F. Inbar, "Patient-driven control of FES supported standing up: A simulation study," IEEE Trans. Rehab. Eng., vol. 36, no. 6, pp. 683–691, 1991.

[46] A. V. Hill, "Then heat of shortening and the dynamic constants of a muscle," Proc. Roy. Soc. Lond., vol. 126, pp. 136–195, 1938. <AU: Kindly provide the issue no.>

[47] N. Lan, "Stability analysis for postural control in a two-joint limb system," IEEE Trans. Neural Syst. Rehab. Eng., vol. 10, no. 4, pp. 249–259, 2002.

[48] R. Riener and T. Fuhr, "Patient-driven control of FES-supported standing up: A simulation study," IEEE Trans. Rehab. Eng., vol. 6, no. 2, pp. 113–124, 1998.

[49] S. Jezernik, R. G. V. Wassink, and T. Keller, "Sliding mode closed-loop control of FES: Controlling the shank movement," IEEE Trans. Bio-Med. Eng., vol. 51, no. 2, pp. 263–272, 2004.

[50] M. Ferrarin, F. Palazzo, R. Riener, and J. Quintern, "Model-based control of FES-induced single joint movements," IEEE Trans. Rehab. Eng., vol. 9, no. 3, pp. 245–257, 2001.

[51] K. J. Hunt, M. Munih, N. N. Donaldson, and F. M. D. Barr, "Investigation of the Hammerstein hypothesis in the modeling of electrically stimulated muscle," IEEE Trans. Bio-Med. Eng., vol. 45, no. 8, pp. 998–1009, 1998.

[52] R. Riener and J. Quintern, "A physiologically based model of muscle activation verified by electrical stimulation," Bioelectrochem. Bioenerg., vol. 43, pp. 257–264, 2007. <AU: Kindly provide the issue no.>

[53] F. Previdi and E. Carpanzano, "Design of a gain scheduling controller for knee-joint angle control by using functional electrical stimulation," IEEE Trans. Control Syst. Technol., vol. 11, no. 3, pp. 310–324, 2003.

[54] R. Happee and F. C. T. V. der Helm, "The control of shoulder muscles during goal directed movements, an inverse dynamic analysis," J. Biomed. Eng., vol. 28, no. 10, pp. 1179–1191, 1995. <AU: Kindly check the name of the second author.>

[55] W. K. Durfee and K. E. MacLean, "Methods for estimating isometric recruitment curves of electrically stimulated muscle," IEEE Trans. Bio-Med. Eng., vol. 36, no. 7, pp. 654–667, 1997.

[56] R. Baratta and M. Solomonow, "The dynamic response model of nine different skeletal muscles," IEEE Trans. Bio-Med. Eng., vol. 37, no. 3, pp. 243–251, 1990.

[57] P. H. Veltink, H. J. Chizeck, P. E. Crago, and A. El-Bialy, "Nonlinear joint angle control for artificially stimulated muscle," IEEE Trans. Bio-Med. Eng., vol. 39, no. 4, pp. 368–380, 1992.

[58] H. J. Chizeck, P. E. Crago, and L. S. Kofman, "Robust closed-loop control of isometric muscle force using pulsewidth modulation," IEEE Trans. Bio-Med. Eng., vol. 35, no. 7, pp. 510–517, 1988.

[59] J. E. Colgate and N. Hogan, "Robust control of dynamically interacting systems," Int. J. Control, vol. 48, no. 1, pp. 65–88, 1988.

[60] E. Langzam, Y. Nemirovsky, E. Isakov, and J. Mizrahi, "Partition between volitional and induced forces in electrically augmented dynamic isometric muscle contractions," IEEE Trans. Neural Syst. Rehab. Eng., vol. 13, no. 3, pp. 322–335, 2006.

[61] J. D. Ratcliffe, J. J. Hatonen, P. L. Lewin, E. Rogers, T. J. Harte, and D. H. Owens, "P-type iterative learning control for systems that contain resonance," Int. J. Adapt. Control, vol. 19, no. 10, pp. 769–796, 2005.

[62] World Health Organisation. (2001). International classification of functioning, disability and health. [Online]. Available: http://www.who.int/classifications/icf/en/

[63] S. Edwards, Neurological Physiotherapy: A Problem-Solving Approach. New York: Elsevier Health Sciences, 2002.

[64] G. Francisco, J. Chae, H. Chawla, S. Kirshblum, R. Zorowitz, G. Lewis, and S. Pang, "Electromyogram-triggered neuromusclar stimulation for improving the arm function of acute stroke survivors: A randomized pilot study," Arch. Phys. Med. Rehab., vol. 79, pp. 570–575, 1998. <AU: Kindly provide the issue no.>

[65] V. S. Huang and J. W. Krakauer, "Robotic neurorehabilitation: A computational motor learning perspective," J. NeuroEng. Rehab., vol. 6, no. 5, pp. 1–13, 2009.

[66] A.-M. Hughes, C. T. Freeman, P. H. Chappell, P. L. Lewin, E. Rogers, J. H. Burridge, M. Donovan-Hall, and B. Dibb, "Stroke participants' perceptions of robotic and electrical stimulation therapy: A new approach," Disabil. Rehab., vol. 6, no. 2, pp. 130–138, 2011.

[67] S. Coote, B. Murphy, W. Harwin, and E. K. Stokes, "The effect of the GENTLE/s robot-mediated therapy system on arm function after stroke," Clin. Rehab., vol. 22, no. 5, pp. 395–405, 2008.

[68] A. J. Doornebosch, H. J. M. Cools, M. E. C. Slee-Turkenburg, M. G. cvan Elk, and M. Schoone-Harmsen, "Robot-mediated ACtive REhabilitation (ACRE2) for the hemiplegic upper limb after a stroke: A pilot study," Technol. Disabil., vol. 19, no. 4, pp. 199–203, 2007.

[69] H. I. Krebs, N. Hogan, M. L. Aisen, and B. T. Volpe, "Robot-aided neuro-rehabilitation," IEEE Trans. Rehab. Eng., vol. 6, no. 1, pp. 75–87, 1998.

[70] C. T. Freeman, D. Tong, K. Meadmore, Z. Cai, E. Rogers, A.-M. Hughes, and J. H. Burridge, "Phase-lead iterative learning control algorithms for functional electrical stimulation based stroke rehabilitation," Proc. Inst. Mech. Eng. I., vol. 225, pp. 850–859, 2011. <AU: Kindly provide the issue no.>

[71] Z. Cai, C. T. Freeman, P. L. Lewin, and E. Rogers, "Iterative learning control for a non-minimum phase plant based on a reference shift algorithm," Control Eng. Pract., vol. 16, no. 6, pp. 633–643, 2008.

[72] T. Lin, D. H. Owens, and J. J. Hatonen, "Newton method based iterative learning control for discrete non-linear systems," Int. J. Control, vol. 79, no. 10, pp. 1263–1276, 2006.

[73] N. Amann, D. H. Owens, and E. Rogers, "Iterative learning control using optimal feedback and feedforward actions," Int. J. Control, vol. 65, no. 2, pp. 277–293, 1996.

[74] K. L. Meadmore, A.-M. Hughes, C. T. Freeman, Z. Cai, D. Tong, J. H. Burridge, and E. Rogers, "Iterative learning mediated FES and 3D robotics reduces motor impairment in chronic stroke," J. NeuroEng. Rehab. [Online]. Available: http://eprints.ecs.soton.ac.uk/ <AU: Kindly update the year if available.>

[75] D. M. Wolpert, Z. Ghahramani, and J. Randall Flanagan, "Perspectives and problems in motor learning," Trends Cogn. Sci., vol. 11, no. 1, pp. 487–494, 2001.

[76] C. T. Freeman, Z. Cai, E. Rogers, and P. L. Lewin, "Iterative learning control for multiple point-to-point tracking application," IEEE Trans. Control Syst. Technol., vol. 19, no. 3, pp. 590–600, 2011.

Callouts:

In response to next generation health care needs there is currently significant interest in both rehabilitation robotics and therapeutic application of FES.

The relationship between reaching and independence is reflected in measures of functional independence, such as the Barthel index where the ability to reach is required for over half of the activity of daily living tasks.

Effective FES-based rehabilitation demands that patients are assisted during functional tasks in a manner that mimics their performance in the absence of impairment.

Iterative learning control is one model-based approach to stroke rehabilitation that has progressed to a program of clinical trials.

Relearning skills after a stroke requires a person to practice movements by repetition and use feedback from previous attempts to improve the next one.